5-1-2018

Processing of Bio-Polymer Based Nanocomposite for Fused Filament Fabrication

Osama Mohammad Khayat
Lehigh University, omk216@lehigh.edu

(Processing of Bio-Polymer Based Nanocomposite for Fused Filament Fabrication)

by
Osama Mohammad Khayat

A Thesis

Presented to the Graduate and Research Committee

of Lehigh University

in Candidacy for the Degree of

Master of Science

in

Polymer Science and Engineering

Lehigh University

May 2018

Thesis is accepted and approved in partial fulfillment of the requirements for the Master of Science in Polymer Science and Engineering Department.

(Processing of Bio-Polymer Based Nanocomposite for Fused Filament Fabrication)

Osama Mohammad Khayat

_____

Date Approved

_____

Thesis Director: Prof. Raymond A. Pearson

_____

Department Chairperson: Prof. Wojciech Z. Misiolek

Acknowledgment

In the beginning, I would like to thank Allah for providing me with physical and mental strength to continue this work and accomplish a master degree from a recognized department in Lehigh University. I would like to thank my beloved parents and siblings for their moral and emotional support during my study.

I would like to express my gratitude to Professor Raymond Pearson for accepting me in the Polymer Group so that I could continue my education in Materials Science and Engineering. I am very thankful for the patience, guidance and knowledge he has shared with me while working on this project.

Special thanks to Gabrielle Esposito for all the help and support she has given me and all the knowledge she shared with me to run every single instrument used in this study. I would also like to thank my Polymer Group; Steve Antalics, Karan Dixit, Caroline Multari, Maria Sartor, Sarah Siddiqui and Tech Tanasarnsopaporn. You have all given me great environment in the office and lab to discuss and share knowledge. I am really thankful for all the time I spent with you.

Finally, I would like to gratefully acknowledge my employer Saudi Aramco/Chemical Business Department for electing me to pursue my graduate studies. Thanks for the financial support and all the work they have put to make my life easier in United states.

Table of Contents

List of Tables

List of Figures

Abstract

Polylactic acid (PLA) is perhaps one of the best known polymers produced from renewable raw materials such as sugar cane and corn starch. Several studies have focused on improving the properties of PLA by incorporating nanofillers in polymer matrix. Cellulose nanocrystals (CNC) is a nanofiller from natural sources (typically wood pulp) that is used to reinforce and modify the mechanical properties and biodegradability of PLA. In this work, cellulose nanocrystals (CNC) reinforced polylactic acid composite was produced in 1, 2, 5 and 10 wt % CNC content by a single-screw extruder in filament form. The effect of cellulose content on the thermal properties of the bio-composite were studied. Differential scanning calorimetry results showed shift in the glass transition temperature and a change in the melting temperatures, where 10% CNC content showed highest reduction in melting temperature. Cellulose proved to increase the crystallinity of the matrix compared to the neat PLA, 1% cellulose exhibited the highest cold crystallization peak. Precision filament (1.75 mm in diameter) was made for fused deposition modeling (3D printing) in order to study the mechanical properties of the bio-composites. The tensile modulus increased in 1% cellulose composites (4.55 GPa) compared to neat PLA (3.03 GPa) for the printed samples. However, the elongation at break reduced when comparing neat PLA (8.7%) while in 1% cellulose was (2.9%).

I. Relevant Literature Review

The environmental awareness has developed dramatically in recent years because of the rising problems in many aspects such as global warming, marine life threats and depleting natural resources. In plastic industry, new direction and interest has been followed to develop environmental friendly and biodegradable products. Polylactic acid (PLA) is one of the most known polymer produced from renewable raw material such as sugar cane and corn starch. Several researches focused on improving and modifying the properties of PLA by incorporating nanofillers in polymer matrix. Cellulose nanoparticle is a natural nanofiller that is used to reinforce and modify the mechanical properties and biodegradability of PLA. In this section I will review several works that focused on preparing PLA/cellulose nanocomposites.

The dispersion of cellulose particles in PLA matrix was studied by Murphy et al [1]. In their work two steps of composite preparation were followed; the first step is film casting and then filament extrusion. Several weight percentages of cellulose were incorporated in PLA (1, 3 and 5 wt/%), each mixture was dissolved in tetrahydrofuran (THF) and put in reaction vessel to stir it at 200 rpm for 90 minutes. The result is completely dissolved cellulose/PLA mixtures which were casted in Petri dish in room temperature for 24 hours. The resulted films were dries and crushed with kitchen grinder to prepare it for extrusion. In Murphy's work, a twin-screw extruder was used to extrude the filaments with 1.55 mm and 1.75 mm which later were used in FDM 3D printing.

Murphy et al [1] characterized the polymer composites using DSC and DMTA. DSC results showed that the glass transition temperature T_g range increases associating with filler

concentration. For neat PLA the T_g curve is sharp compared to other mixtures wither it is modified or unmodified cellulose, Figure [1]. The broad range of T_g indicates that an increase in PLA chain mobility which leads to increasing the crystallinity [1]. For 5 wt/% composites, it is observed that the T_g increased, this could be interpreted as due to the better interaction between cellulose and PLA the molecular motion is constrained [1]. Above observations suggested that filler content of 1 or 3 wt/% helps to increase the crystallinity of the mixture, whereas 5 wt/% filler content drops the crystallinity due to restriction in chain movement.

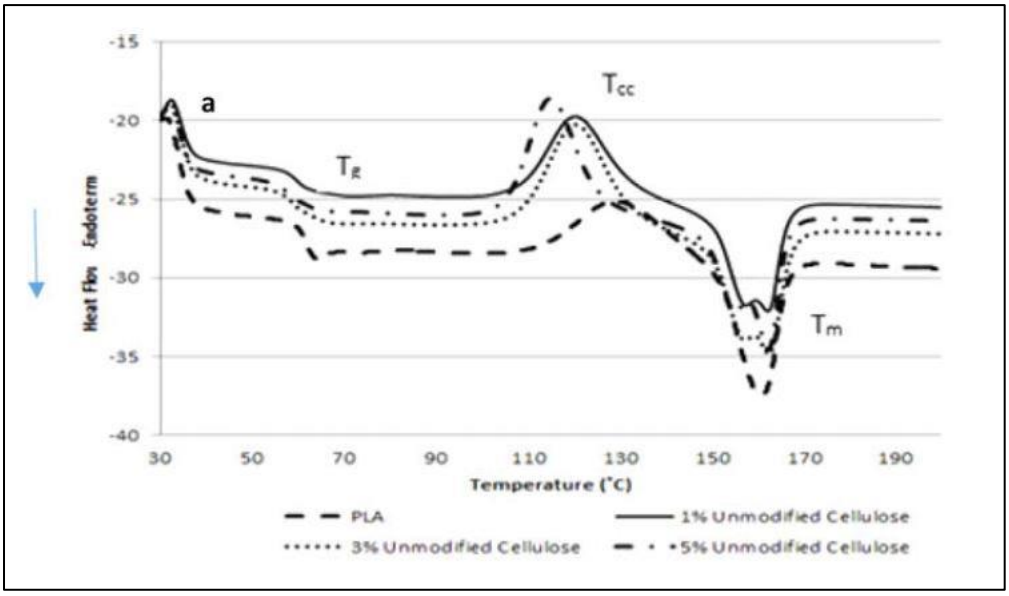

Figure 1: DSC graph of neat PLA with unmodified cellulose [1]

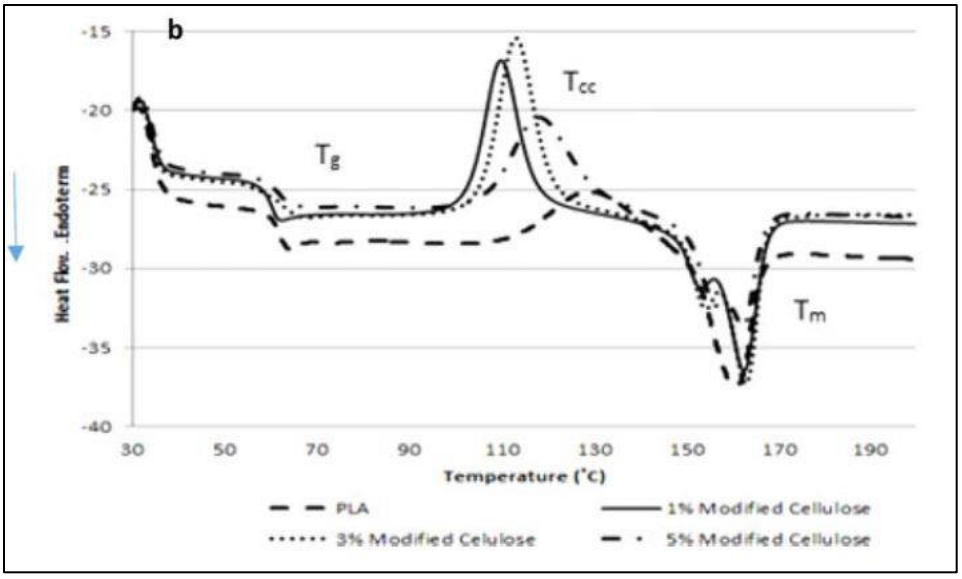

Figure 2: DSC graph of neat PLA and modified cellulose matrix [1]

From Figure [2], the cold crystallinity peaks of modified cellulose look sharper than the neat PLA peak and also shifted to lower temperature, this is an indication of faster crystallization as if the cellulose particles act as nucleation agents [1]. The same behavior is noticed in the modified 1 and 3 wt/% composites, the crystallization peaks shifted toward lower temperature. In 5 wt/% case for both modified and unmodified cellulose the peaks shifted to higher temperature, this is a confirmation to the previous observation that chain motion is restricted which affect the crystallization process.

The DMTA curves in Figure [3] show a reduction in intensity of tanδ peak for 1 and 3 wt/% modified cellulose compared to neat PLA but there was no shift in the temperature, which could be interpret as better dispersion of cellulose in PLA. Whereas tanδ peak of 5 wt/% modified cellulose is shifted to higher temperature indicating better interfacial adhesion between cellulose and PLA [1].

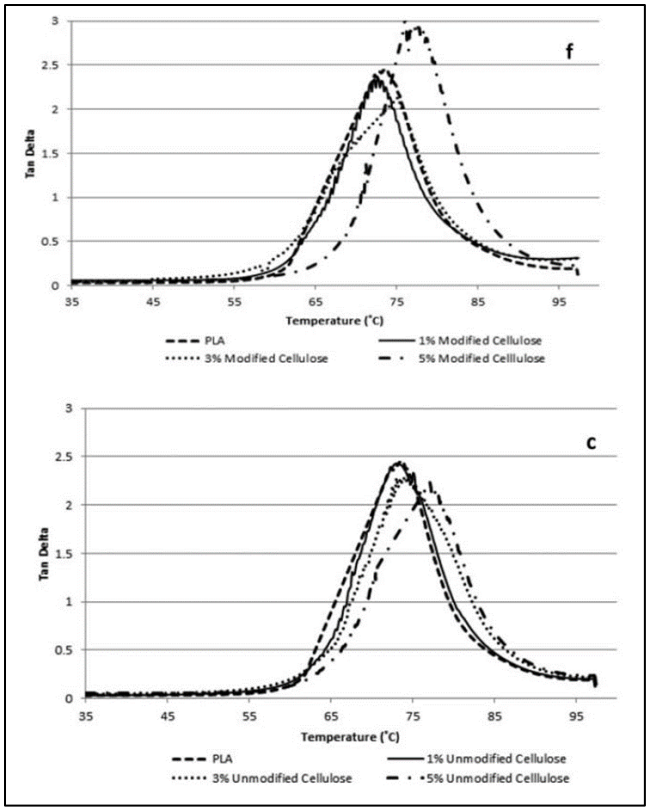

Figure 3: Tan δ peaks of modified and unmodified cellulose composites [1]

For the storage modulus curves in Figure [4], it is noticed that the values of unmodified and modified cellulose at 3 wt/% increased at 35˚C compared to neat PLA. The storage modulus for neat PLA at 35˚C is 2.31 GPa while it is 2.48 GPa for unmodified cellulose and 2.49 GPa for modified cellulose. When looking at the storage modulus values above T_g (~60˚C), the effect of 5 wt/% is bigger than the other mixtures. At 85˚C the value of neat PLA is 4,25 GPa while for unmodified cellulose is 5.88 GPa and for modified cellulose is 5.87 GPa both for 5 wt/%. These results confirm the observations obtained from DSC data that the chain motion is restricted at 5 wt/% in the amorphous region by crystalline cellulose particles [1].

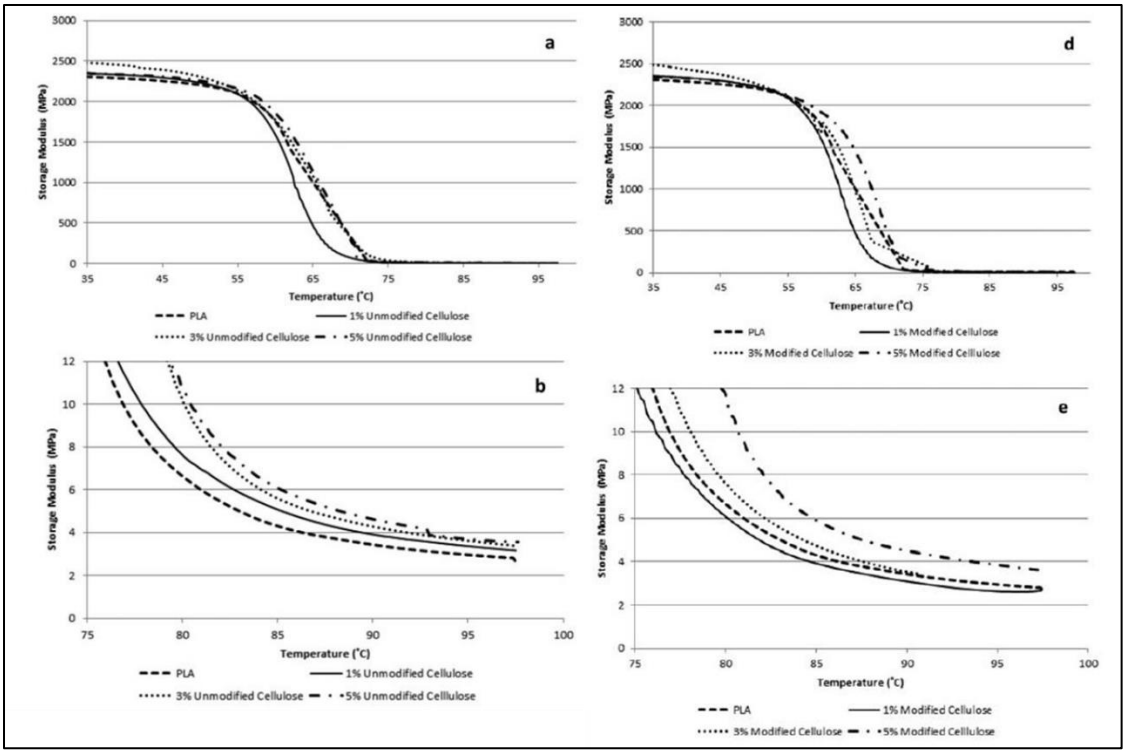

Figure 4: Storage modulus plot of unmodified and modified cellulose bio-composites [1]

Surface modified cellulose nanocrystals were used to prepare nanocomposites of semi-crystalline PLA in the work of Gwon et al [2]. Cellulose nanocrystals (CNC) were modified by acid hydrolysis with sulfuric acid followed by dilution in deionized water. Then CNC suspension was prepared by solvent-exchange with dichloromethane and then dimethylformamide (DMF) in order to prepare it for urethanization process [2]. Afterward, toluene diisocyanate (TDI) was added to the suspension dropwise and another solvent-exchange process conducted where DMF was exchanged with chloroform (CF). Finally, the suspension was sonicated four times each for 15 minutes and homogenous suspension was achieved.

According to Gwon [2], the surface treatment resulted in uneven surface of modified cellulose compared to neat cellulose. The formation of TDI on the surface of cellulose impacted the shape of the nanocrystals as seen in the TEM images in Figure [5].

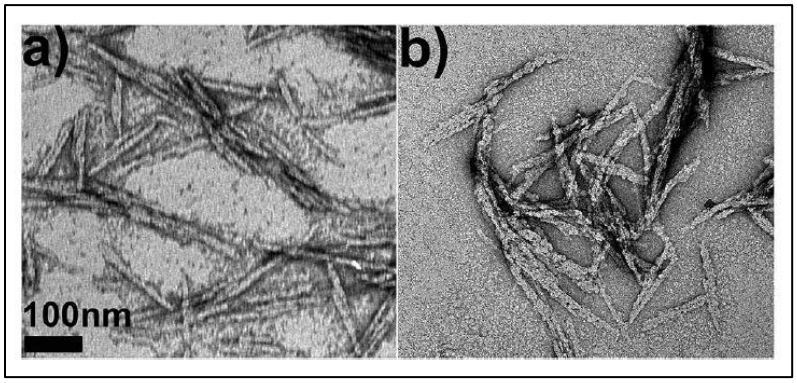

Figure 5: TEM images of a) neat cellulose and b) modified cellulose [2].

Gwon et al observed visually the dispersibility of unmodified and modified cellulose in chloroform, Figure [6]. Both cellulose suspensions consist of 0.01 wt% concentration, the unmodified cellulose started to agglomerate 3 minutes after sonication. In the other hand, modified cellulose maintained its stability. This observation indicates that TDI surface treatment helps to stabilize and improve interfacial compatibility of cellulose nanoparticles.

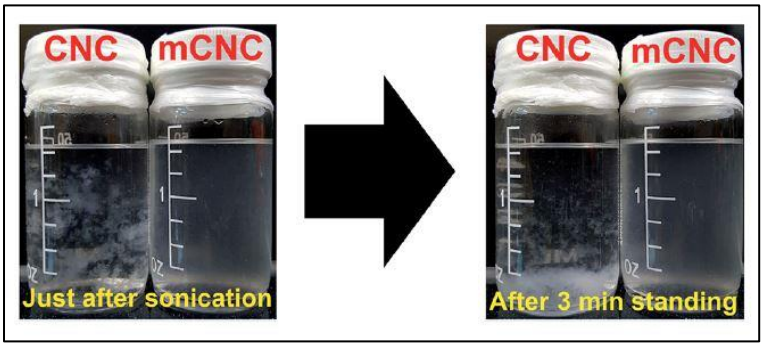

Figure 6: Dispersibility of CNC and modified CNC (mCNC) in chloroform suspensions [2].

The mechanical tensile properties of nanocomposites were tested by Gwon in their study [2]. Two PLA nanofilms were prepared with unmodified and modified cellulose fillers. The tensile strength of unmodified cellulose showed lower values than the modified ones. Gwon concluded that the enhancement in tensile strength is related to the better dispersity of modified cellulose in PLA matrix. The tensile strength values are represented in Figure [7], different grades of PLA (4032D, 3001D and 2003D) were used in Gwon work. The greatest enhancement is noticed in 4032D grade compared to the other PLA grades.

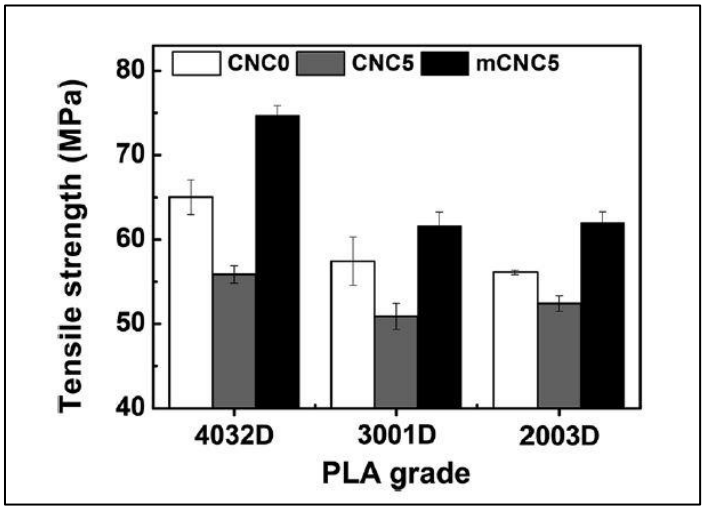

Figure 7: Tensile Strength for different PLA grades with respect to filler content [2].

One of the work of PLA/nanocomposite was done by M. Jonoobi et al. [3], they used cellulose nanofibers to reinforce PLA matrix. Two steps process was done to prepare the PLA nanocomposite; master batch preparation where PLA was dissolved in acetone and chloroform solvent in a ratio of 9:1 by stirring at 55◦C. before that, an acetone-nanofibers suspension was prepared by solvent-exchange of nanofibers with acetone by centrifuging and re-dispersing steps. The PLA dissolved in acetone-nanofiber suspension mixtures were dried, filmed and particulate material was obtained. The second step is melt extrusion by

twin-screw extruder. The extruded PLA nanocomposites were pelletized and dried prior to injection molding to obtain the testing specimens with (1, 3 and 5 wt%) of cellulose nanofibers.

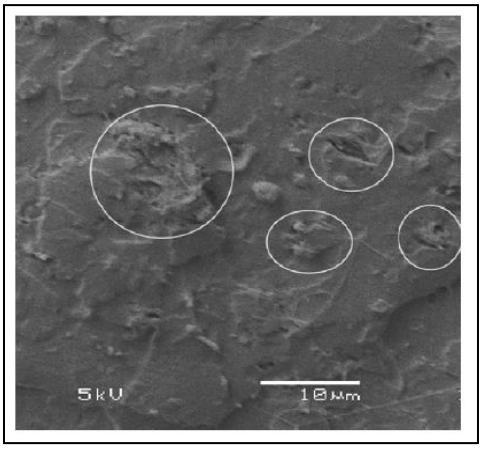

Figure 8: SEM Detailed view of the fractured surface of PLA (5wt%) nanocomposite [3]

The mechanical properties and thermal stability of the nanocomposites were evaluated be several means. SEM images were taken to investigate the surface of the mixtures. Compared to neat PLA, nanocomposites with nanofibers concentration of 1 and 3 wt% showed no significant difference. While in the 5 wt% case, rougher surface was observed where small aggregates of cellulose nanofibers, Figure [8]. SEM images concluded that better dispersion occurs in lower concentrations of nanofibers.

The mechanical properties of PLA nanocomposites tested by tensile testing machine, with load cell of 10 kN and crosshead speed of 3 mm/min. The results indicate that the tensile modulus and strength increases as the filler content increased in PLA. The tensile modulus of neat PLA is measured to be 2.6 GPa, while the measure modulus for nanocomposites was 3.3, 3.4 and 3.6 GPa for 1, 3 and 5 wt% respectively. The same results observed for the tensile strength, neat PLA has a strength of 58.9 MPa while for the modified PLA it

shows 63.1, 65.1 and 71.2 MPa for 1, 3 and 5 wt% respectively. It is worth to mention that high standard deviation was calculated for the modulus and strength data which indicate that the nanofibers were not homogeneously distributed.

The dynamic mechanical properties of PLA nanocomposites were measured using dynamic mechanical analyzer (DMA), Figure [9]. The storage modulus of the nanocomposites increased with respect to filler content. For neat PLA, E' has a value of 2600 MPa at 25◦C while E' for 5wt% nanofiber content value is 4400 MPa at the same temperate. Above the glass transition region (60◦C) the storage modulus is higher for PLA nanofibers than neat PLA as expected, but the difference is quite significant. The storage modulus for 5wt% nanofibers concentration is 2.5 GPa compared to 100 MPa for pure PLA.

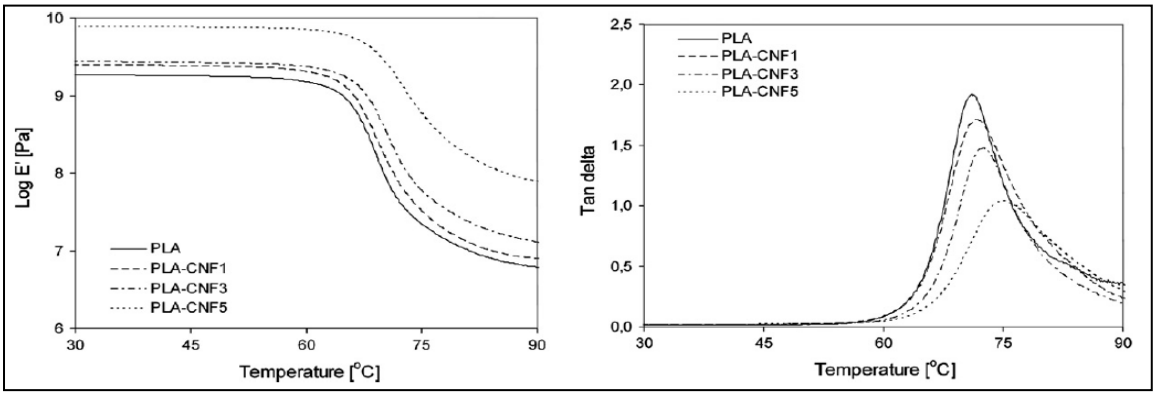

Figure 9: DMA analysis of PLA and PLA nanocomposites; (L) storage modulus and (R) tan δ curves [3].

The tan δ peak was shifted right for the nanocomposites with respect to the filler content. Neat PLA has a peak at 70◦C, the peak is shifted to higher temperature with increasing nanofibers content [3]. As shown in Figure [9], the peak is sharper in pure PLA and gets broader with concentration increase.

In addition to the previous observation in mechanical properties, Jonoobi et al. [3] studied the transparency of the PLA nanocomposites samples. White spots were observed in the samples and it is more visible in 5wt% compared to neat PLA, Figure [10].

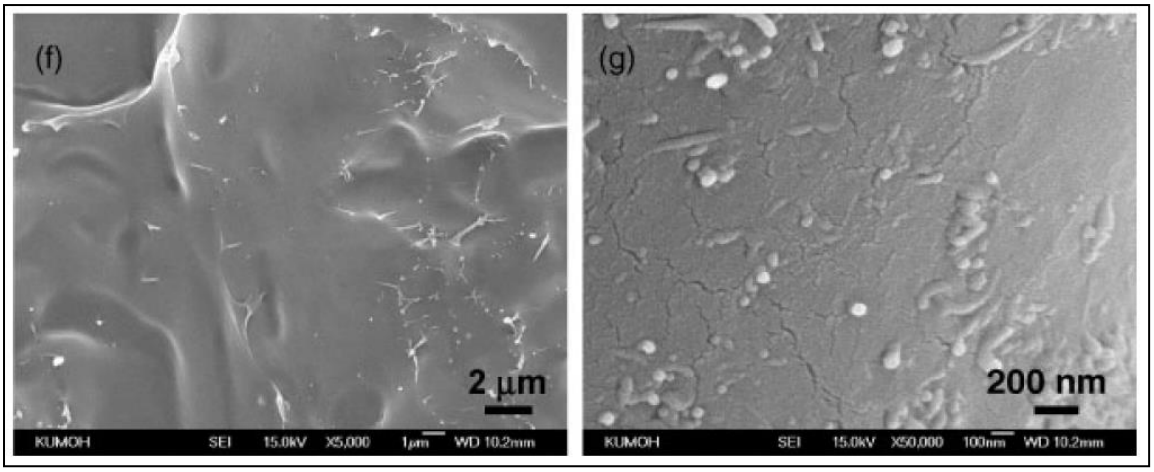

Figure 10: SEM image of PLA/MWNT-g-PLA 5 wt% [3]

Different type of nanofiller was utilized by Oksman et al. [4], they used cellulose whiskers nanofiller to modify PLA matrix. The nanofiller was first prepared by swelling microcrystalline cellulose (MCC) in chemical agent (Dimethyl acetamide) and sonified in ultra-sonic bath to produce cellulose nanowhiskers (CNW). Cellulose whiskers were then fed into twin screw extruder along with the neat PLA to produce the PLA nanocomposite. Compression molding process was carried out to the extruded material to prepare the test samples.

Transition electron microscope was used to study the morphology of the samples. Black dots were observed in the TEM images that indicates un-uniform dispersion of the cellulose nanowhiskers in PLA, Figure [11].

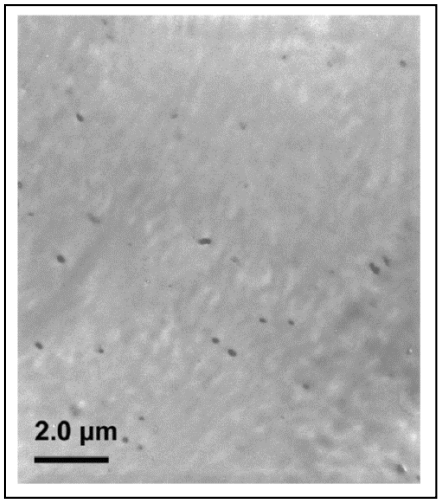

Figure 11: TEM image of PLA/CNW composite [4]

The mechanical properties of PLA/CNW were tested, it was observed that the strength, modulus and elongation at break has been improved. The neat PLA has E modulus of 2.9 GPa, strength of 40.9 MPa and elongation at break of 1.9% while the nanocomposite has modulus of 3.9 GPa, strength of 77.9 MPa and elongation at break of 2.7%. Figure [12] shows the stress-strain curve of both samples and the values are represented in table [1].

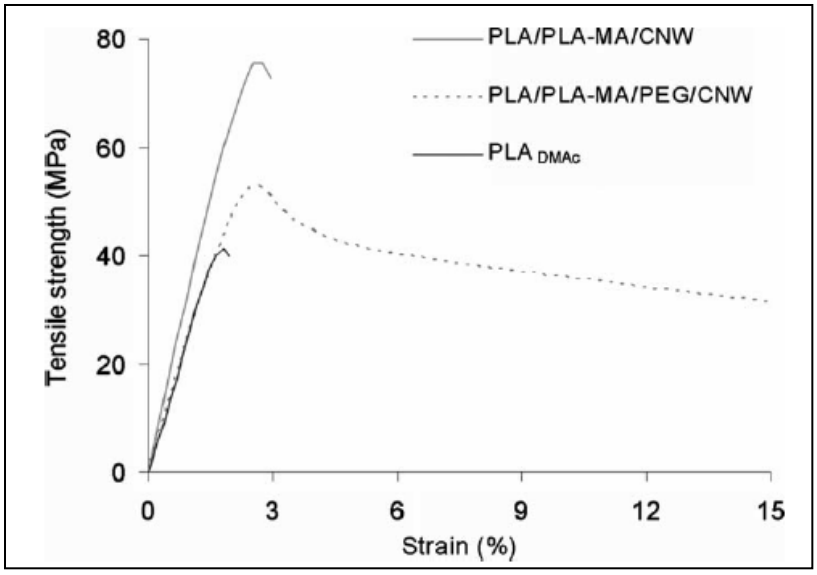

Figure 12: Stress-Strain curve of PLA and PLA/CNW [4]

Table 1: Mechanical Properties of PLA & PLA/CNW [4]

Property	PLA_{DMAc}	PLA/PLA-MA/CNW
E-modulus (GPa)	2.9 (±0.1)	3.9 (±0.3)
Max. strength (MPa)	40.9 (±3.2)	77.9 (±6.7)
Elongation to break (%)	1.9 (±0.2)	2.7 (±0.5)

Recent study conducted by Frone et al [5] investigated the effect of cellulose nanofibers on the crystallinity of PLA matrix. Frone prepared PLA/cellulose matrix with two different cellulose particles based on the surface modification. Unmodified cellulose nanofiber where labeled CN and the surface modified ones were labeled SCN. 2.5 wt% of cellulose particles were added to PLA matrix and mixed by compound mixing method, the same concentration was used for both CN and SCN.

The thermal properties were tested using DSC by Frone [5], DSC results helped to understand the crystallization behavior with respect to nanocomposite concentrations. The results obtained from DSC is presented in Figure [13], the temperature gradient was set to

10˚C/min. Frone noticed a change in T_g in PLA-CN compared to neat PLA and PLA-SCN, the glass transition temperature of PLA-CN is lower because of inhomogeneous dispersion of fibers in the PLA matrix which increased the free volume and the flexibility of polymer chains [5]. The cold crystallization temperature has the most significant effect when cellulose is added especially unmodified cellulose. T_{cc} peak was sharper and shifted to lower temperature compared to neat PLA, which is a result of heterogeneous crystallization. Unmodified cellulose fibers acted as crystallization nucleating agent which resulted in lower $T_{cc..}$ However, the same trend is not shown for the modified cellulose matrix although the same amount of fillers was added. The interfacial compatibility has improved between the SCN and PLA matrix which hindered the crystallization [5]. The enthalpy of crystallization ΔH_{cc} was higher for the nanocomposites compared to neat PLA, this observation supports the idea that cellulose fillers act as nucleating agent for crystallization.

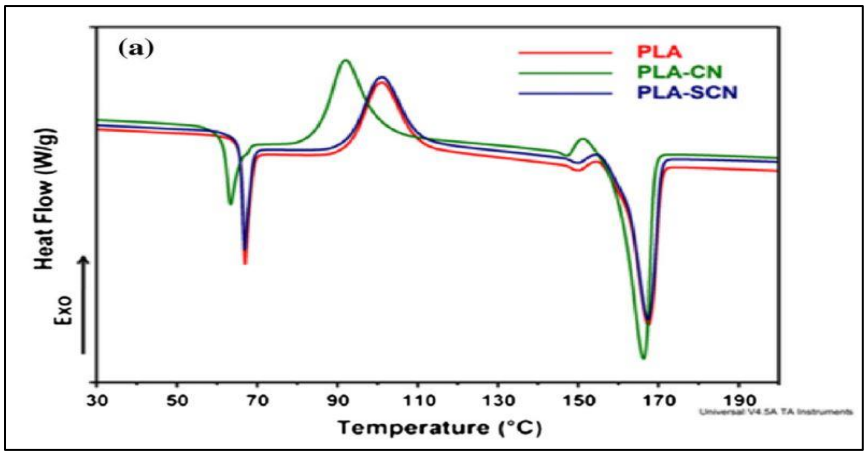

Figure 13: DSC thermograms of PLA and nanocomposites [5]

II. Introduction

Our environmental awareness has developed dramatically in recent years because of the rising problems in many aspects such as global warming, marine life threats and depleting natural resources. In plastic industry, a new direction and interest has emerged for developing environmental friendly and biodegradable products. Polylactic acid (PLA) is one of the most well-known polymers produced from renewable raw materials such as sugar cane and corn starch. Several studies have focused on improving and modifying the properties of PLA by incorporating nanofillers in polymer matrix. Cellulose nanoparticle is a natural nanofiller that is used to reinforce and modify the mechanical properties and biodegradability of PLA. In this study, cellulose nanocrystals (CNC) is used as a natural nanofiller to reinforce semi-crystalline PLA to produce a completely natural polymer-based bio-composite. The aim of this work is to produce such bio-composite filaments using single-screw extruder and to characterize the mechanical properties of these materials using a fused deposition modeling (FDM) 3D printer.

A. Materials

1. Poly Lactic Acid (PLA)

Polylactic acid (PLA) is an aliphatic polyester thermoplastic material. PLA is biodegradable with high rigidity and good optical clarity. As mentioned previously, PLA is produced from renewable sources such as sugar cane or corn starch. PLA can be used in variety of applications such as, medical implant, packaging, food appliances and others. There is much interest in PLA due to its biodegradable properties and there are numerous ongoing studies are to improve the properties of PLA using nanofillers [Garlotta, 6]. PLA-

based nanocomposites experienced an improvement in strength, heat resistance, moduli, degradability and biocompatibility. Also, a decrease in gas permeability and flammability have been observed [Tsuji, 7].

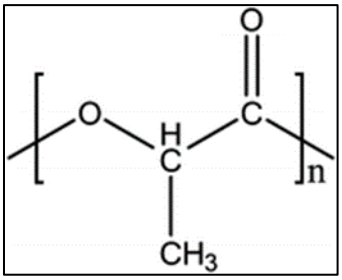

Figure 14: PLA chemical structure

In this work, an extrusion grade PLA was obtained from BLACKMAGIC3D and identified as NatureWorks Ingeo 2003D resin. The differences in the commercial PLA grades offered by NatureWorks involves both the range of molecular weights and the difference sin the ratio of D-lactide to L-lactide isomers. Different ratio of D-lactide to L-lactide affects the ability of PLA to crystallize. NatureWorks does not publically specify the exact ratio of D-to-L lactide in this grade. However, Ingeo 2003D resin was analyzed by [Clark, 8], it has approximately 97 wt% L-lactide and 3 wt% D-lactide. The reported technical specifications of Ingeo 2003D resin is shown in Table [2] below.

Table 2: Ingeo 2003D PLA Properties

Property	Ingeo 2003D PLA
Specific Gravity	1.24
Tensile Strength at Break	53 MPa
Tensile Yield Strength	60 MPa
Tensile Modulus	3.5 GPa

Tensile Elongation	6.0 %

2. Cellulose Nanocrystals (CNC)

Cellulose is a linear polymer chain consists of carbohydrates that is connected by β (1-4) linked in D-glucose units, Figure [15]. Cellulose is a natural substance which considered as one of the most used globally. It is considered as the most abundant organic compound on Earth and has become an important raw material commercially in recent years [Rojas, 9]. Cellulose is found in plant as it is the main material constructing the pants cell wall, also it is found in wood, tunicates, bacteria, etc.

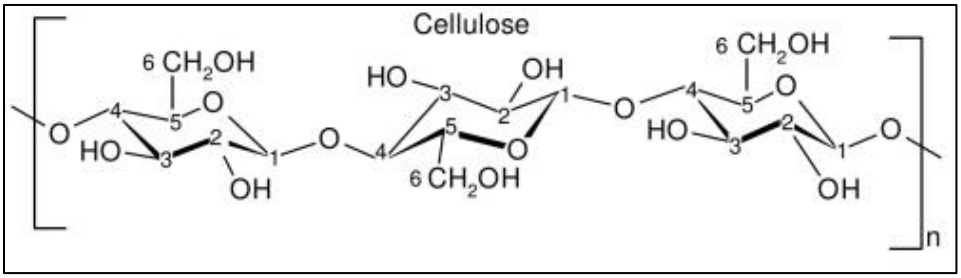

Figure 15: Cellulose Structure

There are several processes that have to be conducted in order to prepare natural cellulose for commercial usage. In this research, cellulose nanocrystals (CNC) was purchased from University of Maine. University of Maine produces two types of cellulose nanoparticles; cellulose nanocrystals (CNC) and cellulose nanofibrils (CNF) [10]. The cellulose is treated with sulfuric acid to hydrolyze the amorphous region, this step produces cellulose crystals resistant to the acid. Purification process takes place after forming the crystals by diluting

and neutralizing the acid, in their labs they use two stages of dilution and setting to remove any contaminants in the cellulose crystals. Afterward, a membrane filtration system is used to ensure pure crystals are obtained. Finally, any water content is removed by another membrane filtration system, slurry cellulose nanoparticles are produced. The slurry product is sold as is or it can be freeze-dried to produce dry powder CNC which is the one used in this work. The specifications and properties of CNC are listed in the table below.

Table 3: Cellulose Nanocrystals Specifications

Test	Specification
Appearance	White, odorless
Solids	98 w/% dry powder
Fiber dimension	5-20 nm wide 150-200 nm long
Density	1.5 g/cm^3
Surface property	Hydrophilic

Cellulose nanoparticles impose excellent mechanical properties which makes it an attractive material to be used as fillers in polymer matrices. However, the investigation of cellulose mechanical properties is challenging because several factors influence the final results [Moon, 11]. These factors include percent crystallinity, crystalline structure, anisotropy, defects, measurement methods and the source of cellulose particles.

The mechanical properties of cellulose nanocrystals have been reported by several works in wide range of values due to the factors mentioned above. The tensile modulus of CNC

is between 105-250 GPa which is comparable to glass fiber (86 GPa), steel wire (207 GPa) (Nishino et al [12], Moon et al [11], Raquez et al [13]).

III. Materials Characterization and Preparation

Polylactic acid, that was described in previous section, was characterized before being processed. The characterization of PLA is important in order to manipulate the process parameters. The molecular weight of PLA was estimated using the dilute solution viscometery method. the extrusion flow rate was calculated as well as the shear rate of the extruder. Also, the rheological properties of PLA were measured using a rheometer.

A. Molecular Weight Measurement of PLA

The viscosity average molecular weight (M_v) of PLA was calculated using dilute solution viscometry method. Dilute solution viscometry measures the viscosity of the polymer by measuring the intrinsic viscosity [η] of polymer solution [Sperling, 14]. Polymer solution was prepared by dissolving 2.0 g of PLA in 100 ml of tetrahydrofuran (THF) to make a 2.0g/dL stock solution. Different concentrations were made by diluting stock solution in THF, the concentrations are 0.25, 0.5 0.75 and 1.0 g/dL. Ubbelohde viscometer uses capillary based method to measure the flow time of the solution. Flow time of solution and solvent are used to calculate the relative viscosity η_{rel} as per the equation [1]

$$\eta_{rel} = \frac{t_{sol}}{t_s} \quad (1)$$

Where t_{sol} is the flow time of the solution and t_s is the flow time of solvent. Another type of viscosity is calculated in this method which is specific viscosity η_{sp}.

$$\eta_{sp} = \eta_{rel} - 1 \quad (2)$$

The relative viscosity is used to calculate the inherent viscosity η_{inh} by equation (3) which is extrapolated to zero to obtain the intrinsic viscosity [η].

$$\eta_{inh} = \frac{\ln(\eta_{rel})}{c} \quad (3)$$

The specific viscosity is used to calculate the reduced viscosity η_{red} by equation (4) which is extrapolated to zero to obtain the intrinsic viscosity [η].

$$\eta_{red} = \frac{\eta_{sp}}{c} \quad (4)$$

The data obtained experimentally was used to plot the inherent and reduced viscosities to extrapolate the intrinsic viscosity, Figure [16]. From the plot, the intrinsic viscosity was estimated to be **1.36015** by taking the average values of the inherent and reduced viscosities. To calculate the viscosity average molecular weight $M_{v,}$ Mark-Houwink-Sakudra equation (5)

$$[\eta] = KM_v^a \quad (5)$$

Where K and a are constants depend on the polymer and solvent at certain temperature. The values of K and a are 5.5×10^{-4} $cm^3.mol^{1/2}/g^{3/2}$ and 0.639 respectively, [Garlotta, 6]. The molecular weight was calculated to be **204272.49** g/mol.

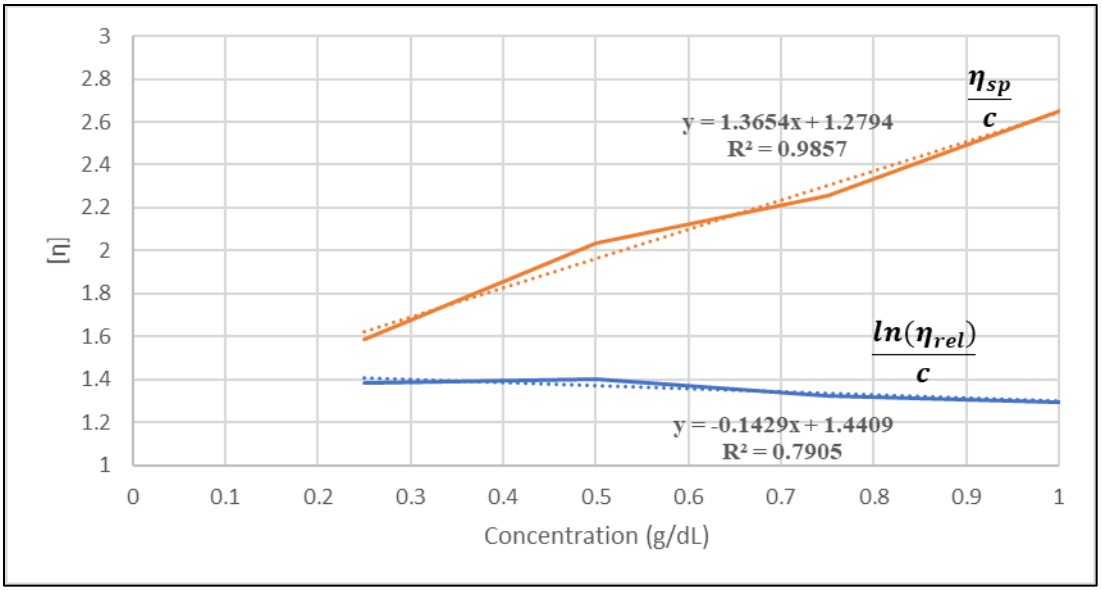

Figure 16: plot of η_{sp}/c and $\ln(\eta_{rel})/c$ versus concentration, and extrapolation to zero concentration to determine $[\eta]$

B. Extrusion Flow Rate and Shear Rate Measurement

The volumetric flow rate (Q) of the extruded polymer was calculated in order to estimate the shear rate of the extruder at certain motor speed. Flow rate measurement was conducted by measuring the weight of extruded material in specific time period (3 min). the volumetric flow rate is calculated by the following equation, $Q = \frac{\dot{m}}{\rho}$. Where $\dot{m}$ is the mass flow rate and ρ is the density obtained from the technical data sheet. Three trials were conducted and the average value of Q was used to calculate the shear rate. All measurements were conducted while maintaining the motor speed at 18 RPM. The measurement data is presented in the following table:

Table 4: Flow rate measurement data

Trial	Time (s)	Weight (g)	$\dot{m}$ (g/s)	Q (cm^3/s)
1	182.37	30.33	0.166	0.134

2	180.50	29.89	0.166	0.134
3	180.20	29.37	0.163	0.131

The average volumetric flow rate is **0.133** cm^3/s.

The shear rate was calculated by equation (6), at motor speed of 18 RPM and temperature set up as 165˚C for the screw, 165˚C for the die and 145˚C for the hopper (these temperatures set up was used in the extrusion process which will be discussed later). At 0.133 cm^3/s flow rate, the shear rate of the extruder equals **0.196** s^{-1}.

$$\dot{\gamma} = \frac{4Q}{\pi R^3} \quad (6)$$

Where $\dot{\gamma}$ is the shear rate and R is the radius of the screw (¾ inch).

C. Polymer composites preparation

The main purpose of this research is to prepare polymer nanocomposites of PLA with CNC. Different weight percentages of cellulose nanocrystals were added to PLA in two forms; pellets and powder. The first attempt of making polymer composites was with PLA pellets which were dried at 80˚C for 24 hours. Cellulose powder was added to the dried pellets and mixed mechanically overnight. The mixture was fed into the extruder hopper, but due to the difference in size between the cellulose powder and PLA pellets it was observed that the powder falls down to the bottom of the hopper first which result in poor mixing. After the first attempt, it was observed that mixing two different shapes and sizes of materials will result in poor mixing and un-uniform filament. To encounter this issue the PLA pellets

was sent to Air Product and Chemicals facility for grinding, PLA pellets were grinded and particles of 200 μm were obtained. After getting the PLA powder, different weight ratio of cellulose to PLA mixtures were prepared. 1, 2, 5 and 10 weight percent of CNC added to PLA and the composites were named PLA-1, PLA-2, PLA-5 and PLA-10 respect to the cellulose content. All materials were mechanically mixed for 24 hours and then dried at 80˚C for another 24 hours to be ready for processing.

D. Melt Rheology Analysis

Rheological analysis of polymer melt gives important information about polymer flow properties which is vital information in processing. Polymer melt rheology was conducted using TA instrument Discovery Hybrid Rheometer (DHR-2), steel parallel plates set up was used to measure the melt viscosity and stress with respect to ramping shear rate at constant temperature. The prepared samples with different cellulose concentrations were tested at two temperatures 160˚C and 170˚C, the shear rate was increased from 0.1 to 10 s^{-1}.

The results for the first test of all samples at 160˚C are shown in Figure [17]. Form the graph, it appears that all samples have steady viscosity for low shear rate, form 0.1 till 1 s^{-1} the viscosity is almost constant. The only different trend is shown in PLA-2, this bio-composite has high viscosity when the test start at about 102 kPa.s but it yields immediately with increasing the shearing rate. This observation suggests that the processing window for PLA-2 is narrow compared to other samples. From the extruder shear rate calculation, the experiment shear rate was 0.196 s^{-1}. At this shear rate, all samples have stable melt viscosity

which allow for good processing conditions except PLA-2 as mentioned before. Another noticeable difference in the results is the low value of PLA-10 viscosity, at low shear rate the viscosity is around 2.3 kPa.s compared to other samples where the viscosity is around 10 kPa.s.

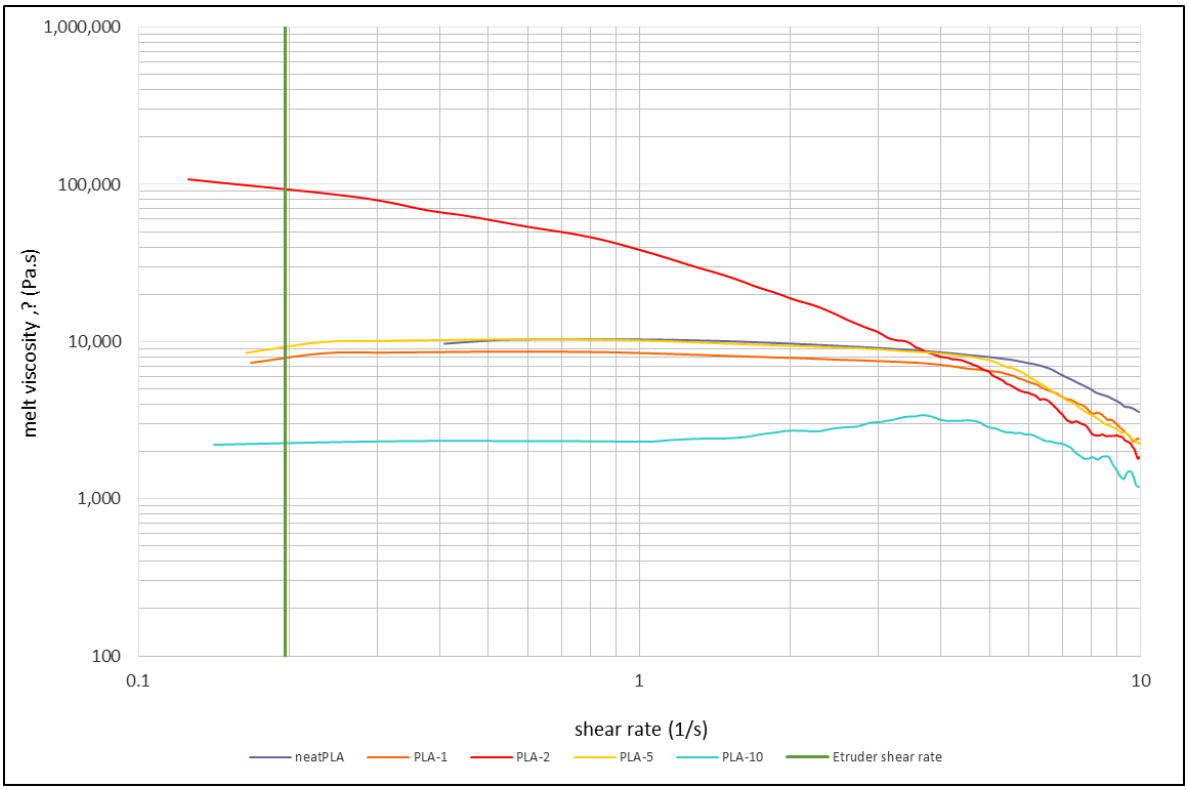

Figure 17: Melt viscosity (Pa.s) vs shear rate (1/s) at 160˚C

The same samples were tested at higher temperature (170˚C), the results are presented in Figure [18]. As expected, the viscosity drops down as the temperature increases, the values show bigger gap among the samples not like at lower temperature. Steadier graph of PLA-2 is observed at 170˚C at lower shear rate. at the extruder shear rate, all samples showed steady and almost constant viscosity which allows for excellent processing condition.

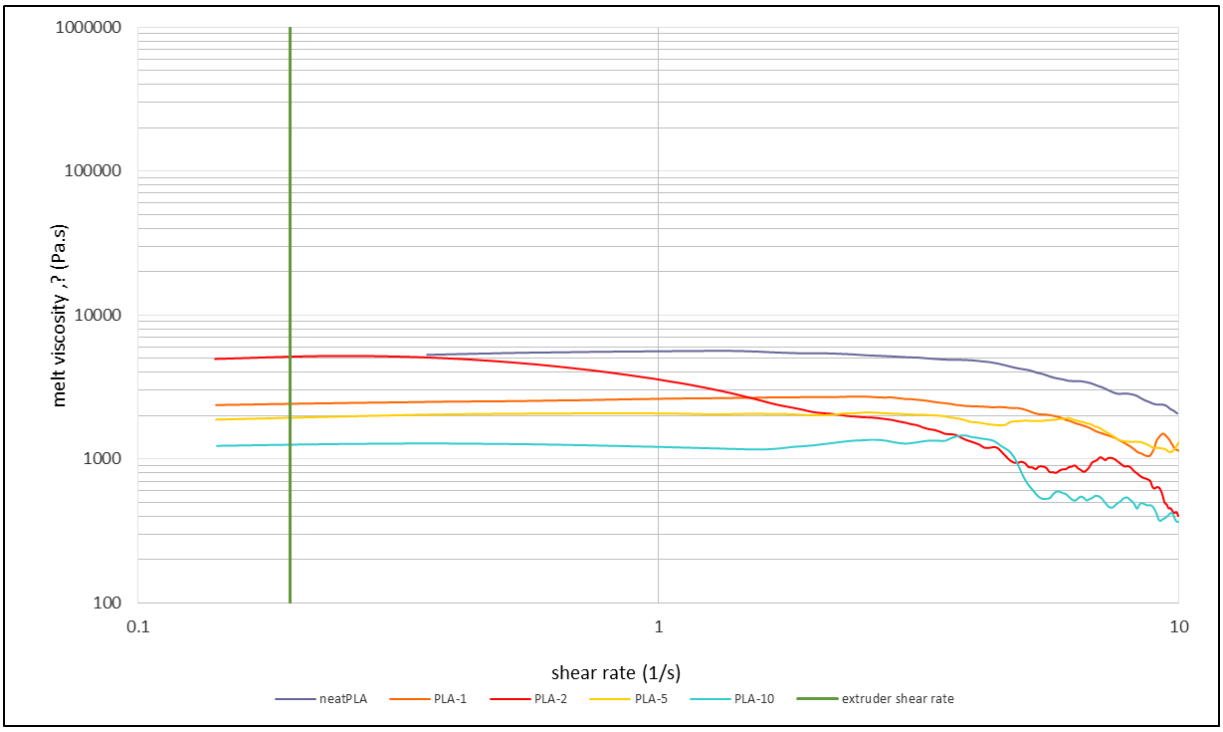

Figure 18: Melt viscosity (Pa.s) vs shear rate (s^{-1}) at 170˚C

IV. Filament Extrusion

In this research, Hot Melt Extrusion (HME) process was used to mix the polylactic acid with cellulose nanocrystals. Hot melt extrusion is a continuous process where heat and pressure are applied to the polymer to melt it and pumped the polymer through an orifice. The main feature of the HME process is that its ability to produce uniform shape and density polymer filament. HME consists of an extruder where the polymer is processed, cooling system to cool down the material extruded and downstream spooler for finalizing the filament spools.

A. Extruder

The main equipment in the HME process is the extruder, a single-screw Branbender Processing Plasti-Corder PL-2000 extruder provided by C.W.Brabender was used in this research. The extruder is equipped with temperature control unit and a motor. The single-screw extruder consists of a hopper used to feed in the polymer, a barrel that contains a ¾ inch single-stage mixing screw of L/D 20:1 to push-down the melted polymer and a 1/8-inch die (orifice) to control the diameter of the filament produced. The extruder has three thermocouples attached to it to control the temperature throughout the process. The locations of the thermocouples are in the hopper, the screw and the die. The temperature is control by auxiliary attached temperature control system supplied by C.W.Brabender as well. A motor is attached to the extruder to control the rotation speed of the screw. Temperature and motor speed can be adjusted online while extruding to obtain the desired filament diameter.

B. Set up and Preparation

The work station set up for the hot melt extrusion process was prepared to produced uniform diameter polymer filament. The lab set up consists of the extruder which was discussed in previous section. Cooling system, in this case a water bath was used to cool down the extruded filament directly after it is pushed out the die. Water cooling helps to harden the extruder filament which makes it easier to process afterward. After the cooling bath the filament goes into an optical micrometer to measure its diameter. The micrometer used in this work was provided by Micro-Epsilon, OptoControl uses the principle of shading or light-quantity measurement to determine the dimension of the filament. The main advantage of the micrometer is that it has the ability to record the measurement and show it while the process is running. This helps to modify and adjust process conditions to obtain better filament quality. Then, Filabot spooler is used to make the final product filament. Filabot spooler allows for fine tuning of filament diameter by adjusting the speed of the draw wheel. It also has a traverse system that distributes the material across the spool to minimize entanglement. The lab set up is shown in Figure [19].

Figure 19: Extrusion set up

C. Results

The hot melt extrusion system described above was used to produce filaments with different weight ratio of CNC to PLA. Temperature control was carried on based on the rheometer results of melt viscosity. The speed of motor for extrusion was modified and adjusted depending on the live measurement of filament diameter through the optical micrometer as well as adjusting the draw speed of the spooler wheel.

Neat PLA (nPLA) was extruded to be used as reference point of measurement and characterization later. The system temperatures were as follow; 145˚C for the hopper, 170˚C for the screw and 170˚C for the die. The motor speed and spooler draw speed was adjusted accordingly. Figure [20] shows the filament diameter as it was extruded, at low motor speed (8 RPM) the diameter was around 1.1~1.4 mm and as the speed increases the desired diameter is achieved (1.7~1.8 mm) at 18 RPM. This diameter range was considered to be the desired diameter based on several attempts in 3D printing which will be discussed later. Figure [21, a] shows a picture of the nPLA filament which appears uniform in shape.

For comparison sake, the diameter of commercial PLA filament was measured via the optical micrometer. As shown in Figure [20], the commercial filament has consistent diameter within the printable range.

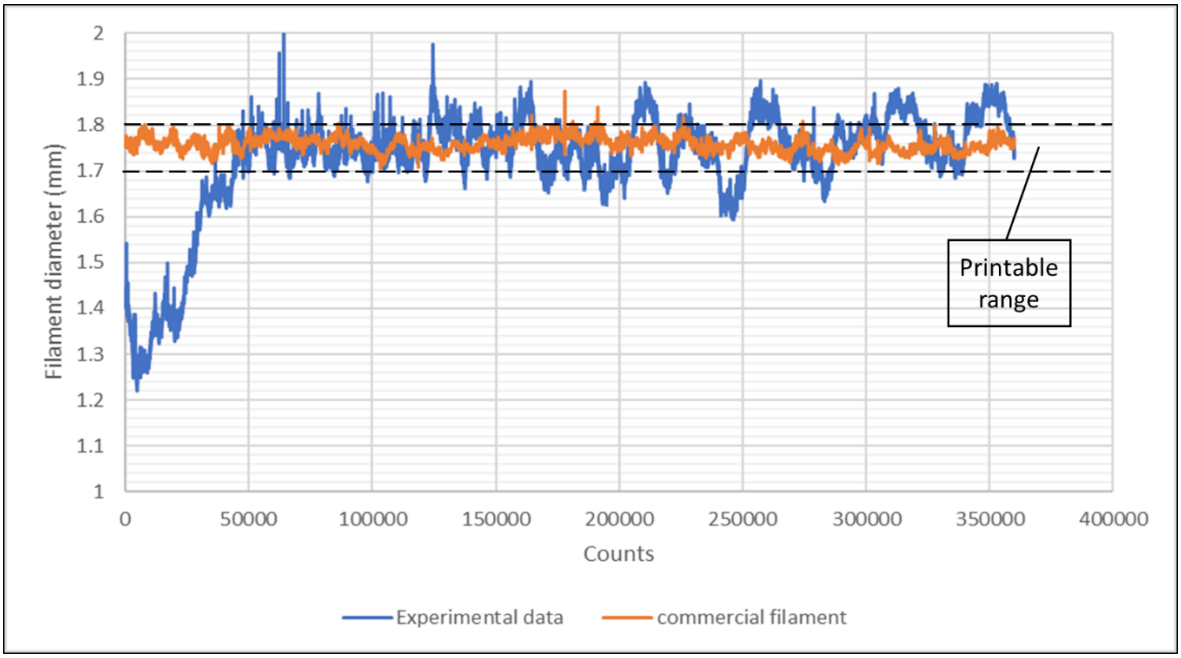

Figure 20: Extruded and commercial filaments diameter recorded by micrometer

The same procedures followed for 1 wt% CNC/PLA composite (PLA-1), parameters were adjusted while measuring the diameter. Two trials were carried on for the PLA-1, the first one resulted in bad shaped filament with a lot of air bubbles captured inside the filament. The most probable reason for this issue is insufficient drying. Cellulose structure contains six hydroxyl group that attract water molecules due to dipole interactions and will thus form hydration shells around them. To encounter this issue, another 1 wt% mixture was prepared and dried at 83˚C overnight. The dried mixture was extruded immediately after getting it out the oven, the set temperatures to obtain decent filament diameter were 140˚C for the hopper, 160˚C for the screw and 160˚C for the die and motor speed was 18 RPM. Extruded PLA-1 filament is shown in Figure [21, b].

The same practice was followed for the other mixtures, they were labeled as PLA-2, PLA-5 and PLA-10 according to the cellulose weight content. The process control parameters for each filament are listed in the table below. The extrusion process for PLA-2 and PLA-5 produced uniform filament while PLA-10 filament has irregular rough surface. The irregular shape of PLA-10 is due to insufficient drying which created air bubbles. The filaments of PLA-2, PLA-5 and PLA-10 are shown in Figure [21, c, d & e] respectively.

Table 5: Conditions used to produce CNC-filled PLA

Composite Name	CNC wt %	Extruder Temperature (˚C)			Motor Speed (RPM)
		Hopper	Screw	Die	
PLA	0	145	170	170	18
PLA-1	1	140	160	160	18
PLA-2	2	145	165	165	18
PLA-5	5	140	165	165	18
PLA-10	10	143	165	165	18

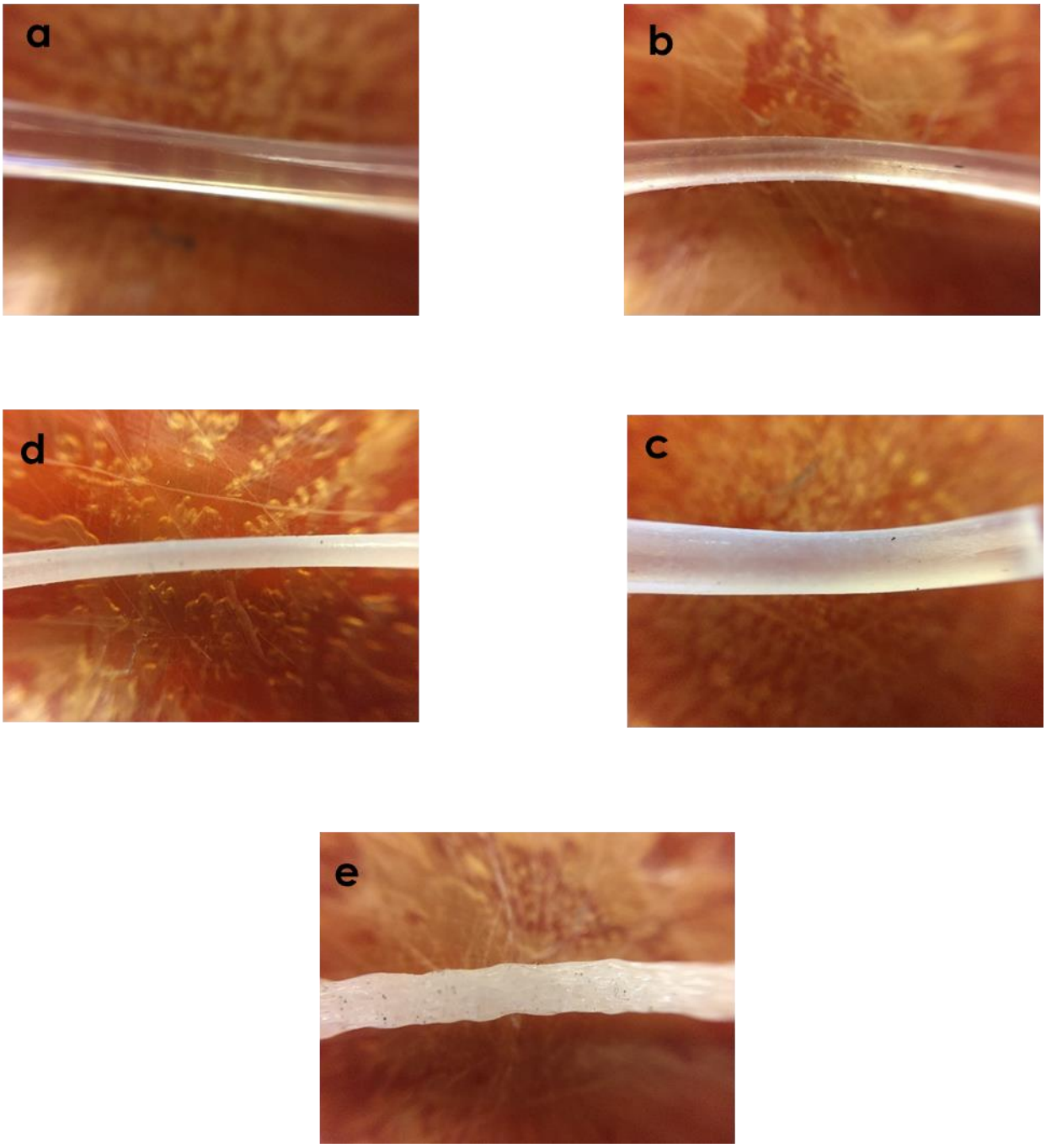

Figure 21: PLA extruded filament, a) neat PLA, b) PLA-1, c) PLA-2, d) PLA-5, e) PLA-10

V. Filament Characterization

Thermal properties and filament composition were examined for the extruded filaments. Thermal properties were studied using differential scanning calorimetry and thermogravimetric analysis. Compositions, in terms of cellulose nanofiller concentration were determined via Fourier transfer infrared spectroscopy. This chapter will discuss the method and results of each of these tests.

A. Differential Scanning Calorimeter (DCS)

In this study, TA Instrument Q2000 Differential scanning calorimeter (DSC) was used to characterize and measure the glass transition temperature (T_g), cold crystallization temperature (T_{cc}), melting temperature (T_m), enthalpy of melting (ΔH_m) and degree of crystallinity (X_c). Each sample was heated up from 25˚C to 200˚C and cooled down to 25˚C at 10˚C/min rate for both heating and cooling. Sample size of 10-15 mg was prepared and placed in aluminum pan and measured while an empty aluminum pan was used as reference point.

All data was obtained directly from the DSC software (Platinum™ Software) except the degree of crystallinity, which is calculated for cold crystallization peak and melting peak by the following equations [7 & 8].

$$X_{c,m} = \frac{\Delta H_m}{\Delta H_{m0}} \times \frac{100}{w} \quad (7)$$

$$X_{c,cc} = \frac{\Delta H_{cc}}{\Delta H_{m0}} \times \frac{100}{w} \quad (8)$$

Where ΔH_m and ΔH_{cc} are the enthalpy of melting and enthalpy of cold crystallization respectively. ΔH_{m0} is the enthalpy of melting of 100% crystalline PLA, which is 93 J/g obtained from (Nam et, [15] al & Ljungberg, [16]). w is the amount of PLA in the sample.

DSC plot of all five composites was generated as heat flow plotted against temperature. The first graph is for the heating cycle and it is shown in Figure [22]. The first peaks in the graph are related to the glass transition temperature (T_g). For all samples the glass transition temperatures are within the range [59 – 63 ˚C]. These values match the reported value in the technical data sheet from NatureWorks. The second peaks are corresponded to the cold crystallization temperature (T_{cc}). The cold crystallization peak of neat PLA occurred at 122.5˚C, the peak is broad and weak as shown in the Figure. The same behavior was observed in cold crystallization peaks of PLA-2, PLA-5 and PLA-10 where T_{cc} range between 115˚C and 125˚C. However, great difference is noticed in the crystallization temperature of PLA-1, this nanocomposite started to crystallize at lower temperature (102.9˚C). Cellulose nanocrystals act as nucleating agent which helped to increase the crystallinity of PLA-1 that appears in T_{cc} peak. The same behavior is not observable in higher concentration of CNC which suggest that at higher concentration CNC particles restrict the motion of polymer chains and prevent crystallization. The area under the curve is used to calculate the degree of crystallinity of polymer, Platinum™ Software gives the value of the enthalpy of crystallization ΔH_{cc} which is plugged in equation (8) to find $X_{c,cc}$. PLA-1 has the higher degree of crystallinity with value of 31.96%. This value is higher than neat PLA where $X_{c,cc}$ is equal to 21.9%. The degree of crystallinity for the other composites is below 20% which is less than the neat PLA. The third peaks are for the melting temperature (T_m), the value of melting temperatures is around 150˚C for all

samples. The only odd value is noticeable at PLA-1 where the polymer melts at 168.6˚C. The cellulose particles in PLA-1 acted as nucleating agents and formed crystallites at lower temperature as mentioned before, and since there is less restriction of motion for polymer chains, these crystallites grew bigger in size and affected the melting temperature. The degree of crystallinity obtained from the enthalpy of melting ΔH_m was calculated using Equation (7). The values of $X_{c,m}$ is slightly higher for PLA-2, PLA-5 and PLA-10. Whereas $X_{c,m}$ for PLA-1 is 43.8% which is almost 11% higher than $X_{c,cc}$.

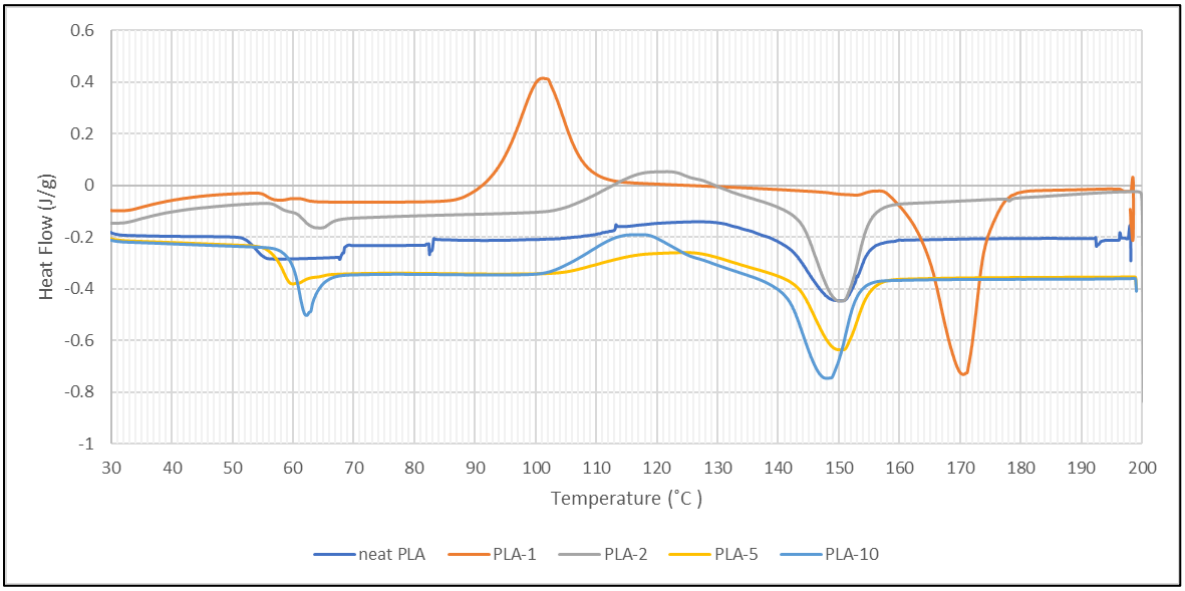

Figure 22: DSC graph of polymer nanocomposites (first heating cycle)

The values obtained from DSC are presented in table [6] as well as the calculated degree of crystallinity.

Table 6: DSC values of Tg, Tcc, Tm, ΔHcc, ΔHm, Xc,cc and Xc,m

	T_g (°C)	T_{cc} (°C)	T_m (°C)	ΔH_{cc} (J/g)	ΔH_m (J/g)	$X_{c,m}$ (%)	$X_{c,cc}$ (%)
Neat PAL	55.59	122.50	148.77	20.41	18.35	19.73	21.95
PLA-1	60.78	102.90	168.60	29.43	40.32	43.79	31.96
PLA-2	62.90	119.18	150.49	15.44	16.73	18.36	16.94
PLA-5	59.25	125.23	150.26	11.91	12.54	14.19	13.48
PLA-10	61.66	115.66	147.95	14.26	18.24	21.79	17.04

The second cycle for the DSC graph is the cooling cycle, the temperature decreased gradually after reaching 200˚C by cooling rate of 10˚C/minutes. The cooling cycle is used to investigate if the polymer will form crystals which will be the maximum crystalline percentage. However, in all experiment samples there were no observative crystallization peaks in the cooling cycles as shown in Figure [23]. The absence of cold crystallization during cooling cycles suggests that the maximum degree of crystallization was already reached and no additional crystallites were formed after the heating cycle. Additionally, the cooling rate (10˚C/min) is too fast to have significant crystallization.

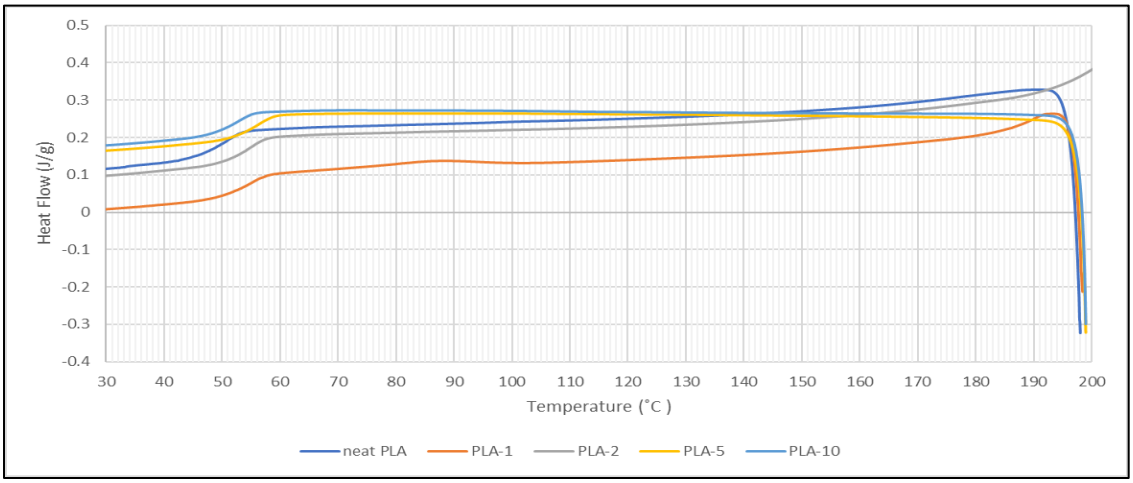

Figure 23: DSC graph of polymer nanocomposites (cooling cycle)

B. Fourier Transform Infrared Spectroscopy (FTIR)

Fourier Transform Infrared Spectroscopy (FTIR) used to investigate the compositions of polymer nanocomposites. The extruded filaments of all bio-composites and neat PLA were studied using PerkinElmer Spectrum 100 FTIR instrument. The samples were tested at room temperature with spectra range from 650 cm^{-1} to 4000 cm^{-1}. Spectra of 5 samples is shown in Figure [24], transmittance (%T) is plotted with respect to wavelength (cm^{-1}).

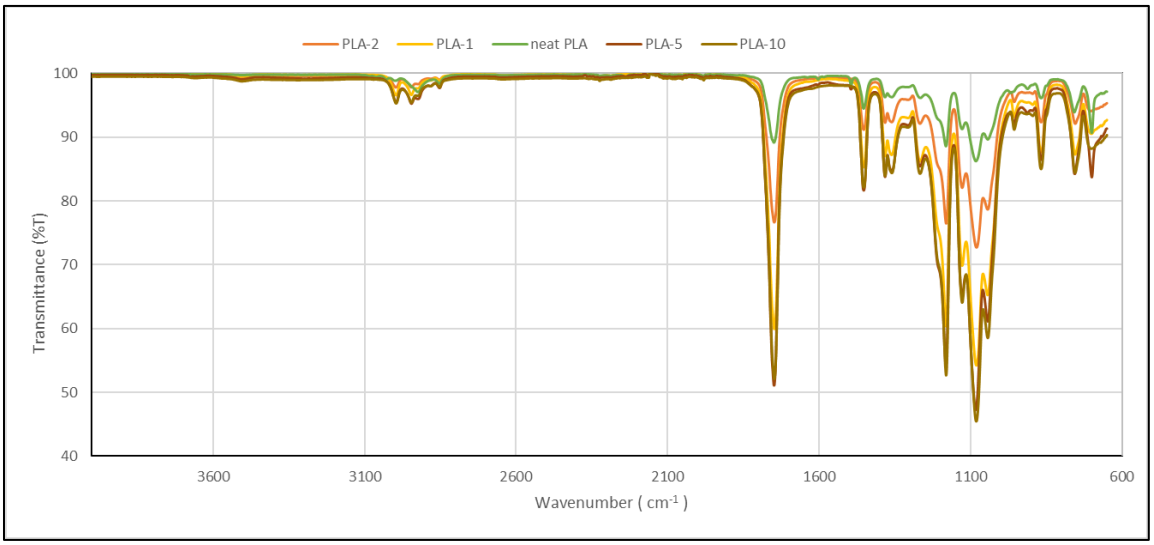

Figure 24: FTIR spectrum of nanocpmposites

From the graph, the first observable difference in data is the intensity variation of the peaks. The intensity of the peaks increases as the concentration of cellulose increases in PLA matrix. Although almost all peaks are at the same wavelength, the peaks at PLA-10 are stronger. As the concentration decreases the peaks get weaker. This gives an indication that the nanocomposite preparation was sufficient and the extrusion process was successful to incorporate the nanoparticle in polymer matrix.

To break down the graph, the peaks at 2996 cm^{-1} are related to the O-H intramolecular bond stretching. The peaks at 2924 cm^{-1} are associated with C-H alkane bond stretching.

The peaks at 1750 and 1180 cm^{-1} are the ester bonds stretching of C-O and C=O of PLA. The methyl group in PLA ($-CH_3$) has peaks at 1450 cm^{-1}. The primary and secondary alcohol groups in cellulose have peaks at 1043 cm^{-1} and 1081 cm^{-1} respectively. The peaks at the range from 700 to 900 cm^{-1} are for the alkane C-H bonds bending. [Tserki,18]. The absorption peaks and their corresponding bond types are represented in the table below.

Table 7: FTIR absorption peaks and corresponding bonds type

Absorption (cm^{-1})	Bond	Type of Bond	Remark
~2996	O-H	Intramolecular bond	stretching
~2924	C-H	Alkane	stretching
~1750	C=O	Ester	Stretching
~1450	$C-H_3$	Methyl group	Bending
~1359	O-H	Alcohol	Bending
~1180	C-O	Ester	Stretching
~1081	C-O	Secondary alcohol	Stretching
~1043	C-O	Primary alcohol	stretching
700~900	C-H	Alkane	Bending

C. Thermogravimetric Analysis (TGA)

The processability of PLA nanocomposite in term of temperature range can be studied using thermogravimetric analysis (TGA). In TGA test, bio-composites weight loss is measured with respect to temperature increase. The test was carried out using TA instrument TGA Q500, the samples were heated from 30˚C to 700˚C with heating rate of

10˚C/min. different polymer composites samples were tested with different weight percent of cellulose content as well as pure CNC sample for comparison.

The test results are presented in Figure [25], the residual weight percent is plotted against temperature. All materials are thermally stable till temperature reached 230˚C where the weight of the samples started to decrease [Petersson, 18]. This result indicates that the processing window for these polymer nanocomposites can be as high as 230˚C, which gives a wide process window for 3D printing at temperature up to 230˚C, the materials lost less than 1% of its weight. Another information obtained from TGA graph is the decomposition of bio-composites. PLA-1 and PLA-2 completely decomposed at lower temperature (360˚C), while PLA-5 and PLA-10 decomposed totally at around 380˚C. Higher cellulose concentration may have acted as physical crosslinking agent led to more entanglements in the matrix that affected the decomposition temperature.

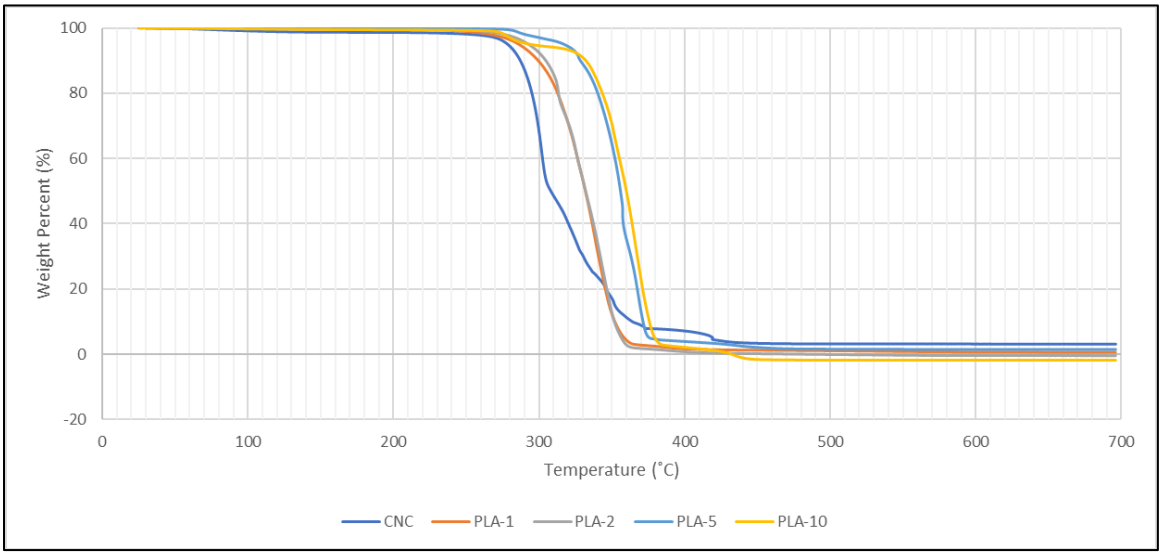

Figure 25: TGA graph of different bio-composites

VI. Fused Deposition Modeling (FDM) 3D Printing

In this work fused deposition modeling (FDM) 3D printer was used to print and test the extruded filament. FDM is the wildly most used 3D printing process that uses thermoplastic filament, mostly PLA or ABS. the filament is heated to the melting point and then extruded layer by layer to make 3D objects.

A. Lulzbot TAZ 5

The FDM 3D printer used in this work was Lulzbot TAZ 5, which uses 3.0 mm or 1.75 mm filament diameter. The printer features a modular head where the filament is fed, the head controls the printing speed through a motor. The filament is heated in a hot-end equipped with temperature control and extruded through 0.35 mm nozzle. TAZ 5 has a heated print surface that is used in keeping the extruded plastic warm and thus preventing warping. Warping is the issue when the edges of the printed plastic cools prior to the rest of the object and fold toward the center which deform the object.

B. Filament Printing Troubleshooting

During the printing process, several issues were faced that affected the printed objects quality or malfunctioned the 3D printer itself. In this work, commercial PLA filament was used to compare the quality of the printed objects with the filaments extruded in the lab. The main issue that has been observed during the process is associated with filament quality and diameter which affected the printed objects and the printer hot-end head and nozzle.

As mentioned before, some air bubbles were noticed in PLA-10 and PLA-5 due to insufficient drying of PLA matrix. In the printing process when a filament with air bubbles

was used, it was observed that there is an interruption in filament extrusion from the nozzle. This inconsistency leaves gaps in the printed objects which affect the quality of it.

The other problem encountered while printing is the filament diameter inconsistency. Lulzbot Taz 5 uses a plunger to apply pressure to filament and a driving gear that push the filament down to the hot-end, Figure [26]. In normal operation, the plunger pins the filament to the driving gear by pressure that is adjusted by screws depending of the filament diameter. The pinned filament is dragged by the gear teeth and pushed to the hot-end [Chilson, 19]. The plunger tension is adjusted before start printing to make sure filament extrusion is smooth and continuous. However, if the filament diameter is irregular the applied tension, which is adjusted manually, may vary during the process. This problem was experienced during the printing of the extruded filament, as shown in Figure [20], there is some fluctuation in the diameter of the extruded filament. As a result, the filament is not dragged into the hot-end and filament residue is left inside the nozzle. Subsequently, the residue cools down and clogs the pathway that can only be cleared out by dismantling the whole printing head.

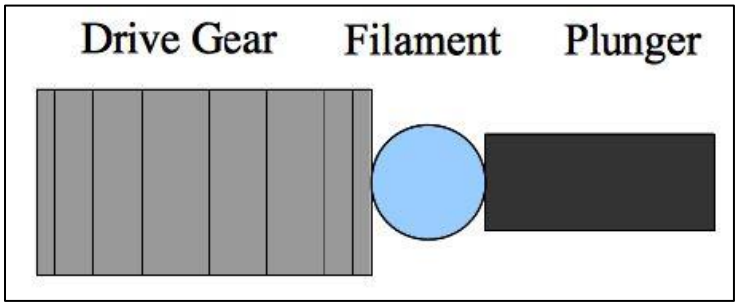

Figure 26: TAZ 5 driver gear and plunger set-up [19]

To encounter this issue, several trials with different diameters have been conducted to evaluate the appropriate filament diameter range that can be printed without

malfunctioning the 3D printer. The printable diameter range was estimated to be 1.70-1.80 mm, within this range the driver gear was noticed to work efficiently and was able to grab the filament properly without the need to adjust the plunger tension. When the diameter is below ~1.70 mm, the filament becomes loose because there is no enough pressure from the plunger and the gear teeth cannot push the filament toward the nozzle. Eventually the printed object will deform because there is no filament extruded out the nozzle. On the other hand, if the diameter is larger than ~1.80 mm, the filament will be too thick and stick in the channel toward the hot-end and lead to the same problem (clogging).

VII. Mechanical Properties of 3D Printed Objects

In order to test the mechanical properties of the extruded filament, Lulzbot TAZ5 was used to print tensile samples and dynamic mechanical analysis (DMA) samples. However, since there is fluctuation in filament diameter during extrusion, not all prepared filaments were printable. As shown before in Figure [21], PLA-10 filament is irregular in shape which caused troubles while printing. The dog-bone samples of neat PLA, PLA-1 and PLA-5 were successfully printed as well as DMA samples of neat PLA, PLA-1, PLA-2 and PLA-5.

A. Tensile Properties

The tensile properties of cellulose modified PLA bio-composites were tested according to ASTM-D638-10 standard. The standard test method requires 5 tensile samples per test and an average value to be reported. The sample type used in the test is Type-V with dimension of 3.18±0.03 mm width, 9.53±0.08 mm length and 3.2±0.04 mm thickness. The test was conducted using tensile testing machine (Instron 5567).

Test results of neat PLA samples showed tensile modulus of 3.03 GPa which is less than the value reported in the technical data sheet (3.5 GPa). The reduction in Young's modulus is due to the shear applied to PLA during extrusion while filament making and printing. The same reduction is observed in tensile yield, where the technical data reported 60 MPa while the measured value of neat PLA is 51.4 MPa. The elongation at break of neat PLA is 8.7% while the raw material data is 6.0%.

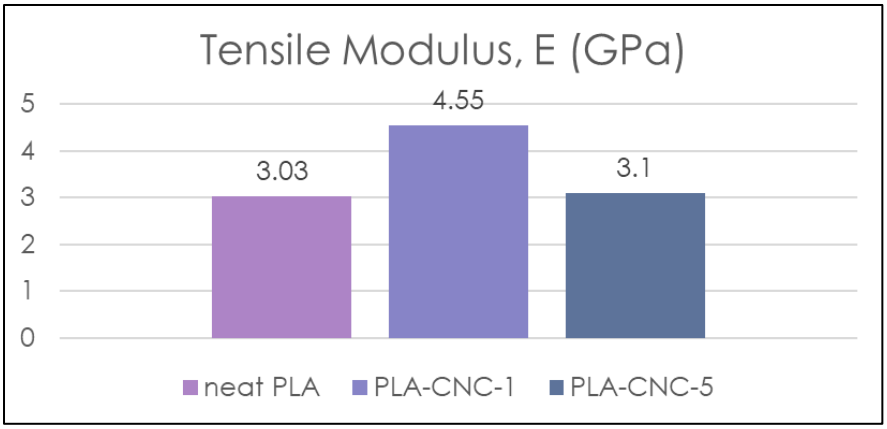

Figure 27: tensile modulus of printed samples

For the nanocomposites results, PLA-1 results show improvement in tensile data compared to neat PLA. The tensile modulus increased by 50% where the value of PLA-1 is 4.55 GPa while the neat PLA has a value of 3.03 GPa, Figure [27]. The yield strength also improved from 51.4 MPa in neat PLA to 61.1 MPa in PLA-1. However, a drop in the strain at break was observed in PLA-1 (2.8%) while the neat PLA sample value is 8.7%, Figure [29]. The improvement in tensile properties indicates that cellulose particles oriented in the polymer chains direction which allow it to absorb the load. The bio-composites are stiffer than the neat plastic but the increase of stiffness is in the cost of strain.

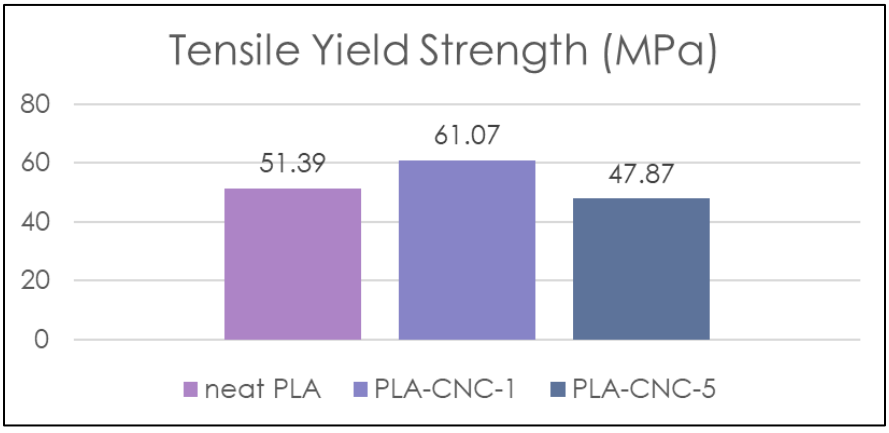

Figure 28: yield strength of nanocomposites

On the other hand, the tensile properties dropped in almost all properties for PLA-5. The tensile modulus is the same as the neat PLA (around 3.0 GPa) as shown in Figure [27]. Where the yield strength dropped by 8%, 51.4 MPa for neat PLA compared to 47.9 MPa for PLA-5, Figure [28]. The difference in elongation at break for PLA-5 is better compared to PLA-1 with respect to neat PLA, PLA-5 strain at break value is 4.4% which is almost 50% reduction than neat PLA. The reason why tensile properties decreased for PLA-5 is that the nanocrystals did not disperse well in the matrix, the orientation of crystals are not aligned with the polymer chains direction.

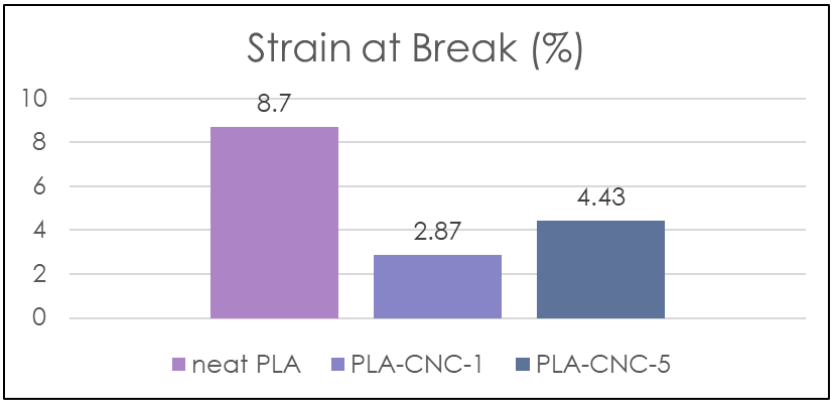

Figure 29: elongation at break data for nanocomposites

B. Halpin-Tsai model for tensile modulus prediction

The reinforcement of fillers on polymer matrix can be measured by a model developed by Halpin-Tsai. In Halpin-Tsai model, the theoretical modulus of the composite is calculated based on the modulus of the polymer and the filler. The model takes into account the filler

volume fraction as well as the geometry of the filler. The values of Halpin-Tsai model will be compared with the experimental values obtain from Instron tensile tests.

The model calculates the theoretical composite modulus E_c using the following equations,

$$\frac{E_c}{E_m} = \frac{1+\zeta\eta\Phi}{1-\eta\Phi} \quad (9)$$

$$\eta = \frac{{E_f}/{E_m} - 1}{{E_f}/{E_m} + \zeta} \quad (10)$$

Where E_c is the composite modulus, E_m is the polymer modulus, E_f is the filler modulus. Φ represents the volume fraction of the filler. ζ is a parameter signifying the aspect ratio of the filler, assuming two different shapes of the nanocellulose, the first is spherical shape and the second is whiskers. The value for E_m is taken from the technical data provided from NatureWorks (3.5 GPa). The value for E_f is taken from different sources since there is a wide range of values reported in literature, each value will be presented associated with its source. The volume fraction Φ is calculated based on the weight percentage of CNC in the matrix. volume fraction Φ is calculated by the following equation:

$$\Phi = \frac{(\frac{w_r}{\rho_r})}{(\frac{w_r}{\rho_r}) + \frac{(1-w_r)}{\rho_m}} \quad (11)$$

Where w_r is the weight percentage of CNC in PLA matrix, ρ_r and ρ_m are the density of CNC and PLA respectively. Density values were taken from the data sheet of both materials.

The predicted values from the model with respect to cellulose tensile modulus source is shown in Figure [30] as well as the values obtained from the experiment in section V.A.

the first data set is calculated based on the spherical shape fillers, the value of ζ is 2 in this assumption. An important thing to consider regarding Halpin-Tsai model is that the model assumes fully dispersion of nanofillers in the matrix, and the nanoparticles are aligned in the longitudinal direction and have perfect interfacial adhesion to the matrix [Jonoobi et al, 3]. The experiment data does not match the calculated value of the model, keeping in mind that only neat PLA, PLA-1 and PLA-5 were tested. The results shown in Figure [30] indicate that the cellulose particles are not aligned in the longitudinal direction and they are randomly dispersed in the matrix. Also, the lower value of experimented PLA-5 suggests poor dispersion of CNC and it might agglomerate in PLA composite.

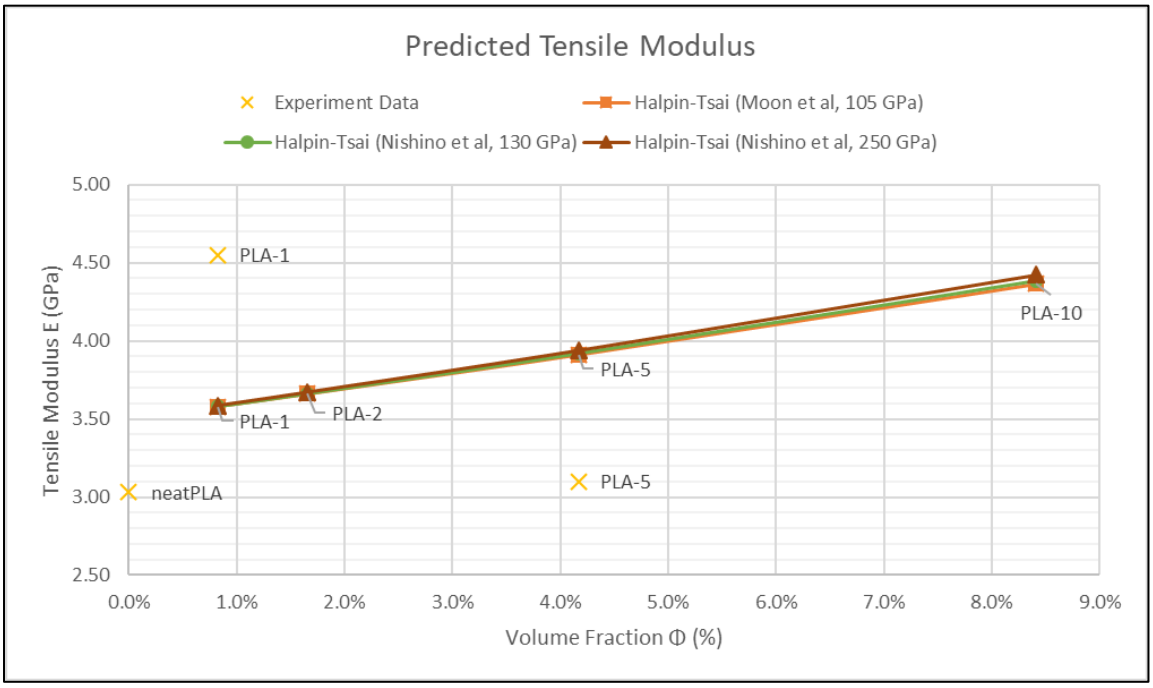

Figure 30: Halpin-Tsai model for nanocomposite tensile modulus prediction (ζ=2)

The second data represents the values of Halpin-Tsai model calculated while considering whiskers fillers. ζ in this case is calculated based on the length to diameter ratio, the

equation is $\zeta = 2 * \frac{l}{d}$ where the length and diameter values were obtained from the average value in the technical data sheet. In this case, ζ = 2*(175/12.5) = 28. Another assumption associated with the filler shape is the assumption that fillers are randomly distributed. Cellulose whiskers are taken both configuration, wither it's aligned in the polymer chain direction or perpendicular to it. Figure [31] shows the values with respect to different cellulose nanocrystals modulus depending on the source. From the plot, it is shown that the estimated values at PLA-1 are almost matching the measured values by tensile test. However, the value is increasing drastically with the increasing of volume fraction which indicates that the model is not accurate when assuming whiskers shape nanofillers.

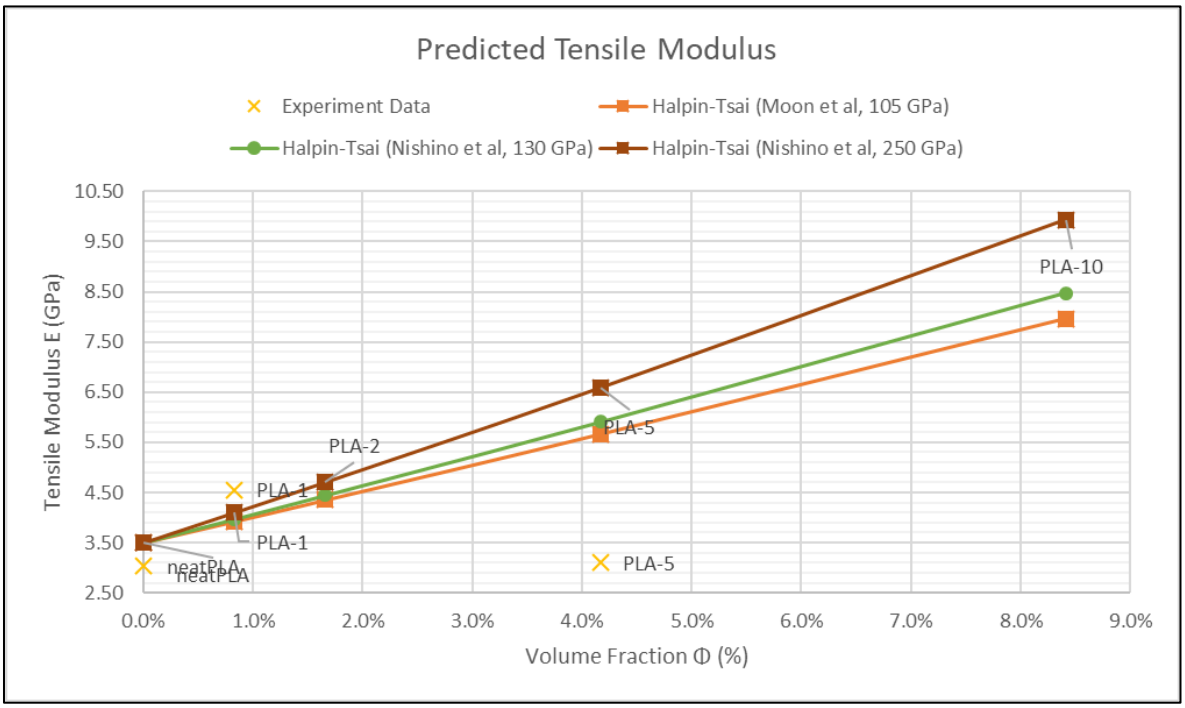

Figure 31: Halpin-Tsai model for nanocomposite tensile modulus prediction (ζ=28)

C. Dynamic Mechanical Analysis (DMA)

Dynamic Mechanical Analysis, otherwise known as DMA, is a technique where a small deformation is applied to a sample in a cyclic manner. This allows the materials response to stress, temperature, frequency and other values to be studied. DMA data helps to understand the plastic and elastic behavior of polymers. In this work, the dynamic mechanical analysis was conducted using TA Instrument Discovery Hybrid Rheometer (DHR-2).

DMA test was conducted based on ASTM E-2254 test method for storage modulus and loss modulus. The sample for DMA tests is a rectangular shape specimen with dimensions of 13x3x52 mm for width, thickness and length respectively. The test was conducted at temperature range from 25˚C to 140˚C with temperature ramp rate of 1˚C/minute. The frequency of oscillation was set to 1.0 Hz. Neat PLA, PLA-1, PLA-2 and PLA-5 sample were used for DMA, PLA-10 filament was difficult to print due to its irregular shape. The storage modulus E', loss modulus E" and tan δ values were measured from this experiment.

The storage modulus E' data is represented in Figure [32], the neat PLA has a storage modulus value of 0.68 GPa at 30˚C, which is below the glass transition temperature. An improvement is noticed for the value of PLA-1 and PLA-2, at 30˚C the values are 1.06 and 0.95 GPa for PLA-1 and PLA-2 respectively. However, the storage modulus for PLA-5 value is the lowest among all samples, PLA-5 has storage modulus of 0.62 GPa. These values indicate that the lower concentration of cellulose in the matrix acts better in aligning the particle in the orientation of polymer chains direction. Higher concentration in PLA-5 lead to poor dispersion on nanoparticles in PLA matrix and that affected the mechanical

properties. Figure [32] below shows the plot of storage modulus as function of temperature for four samples.

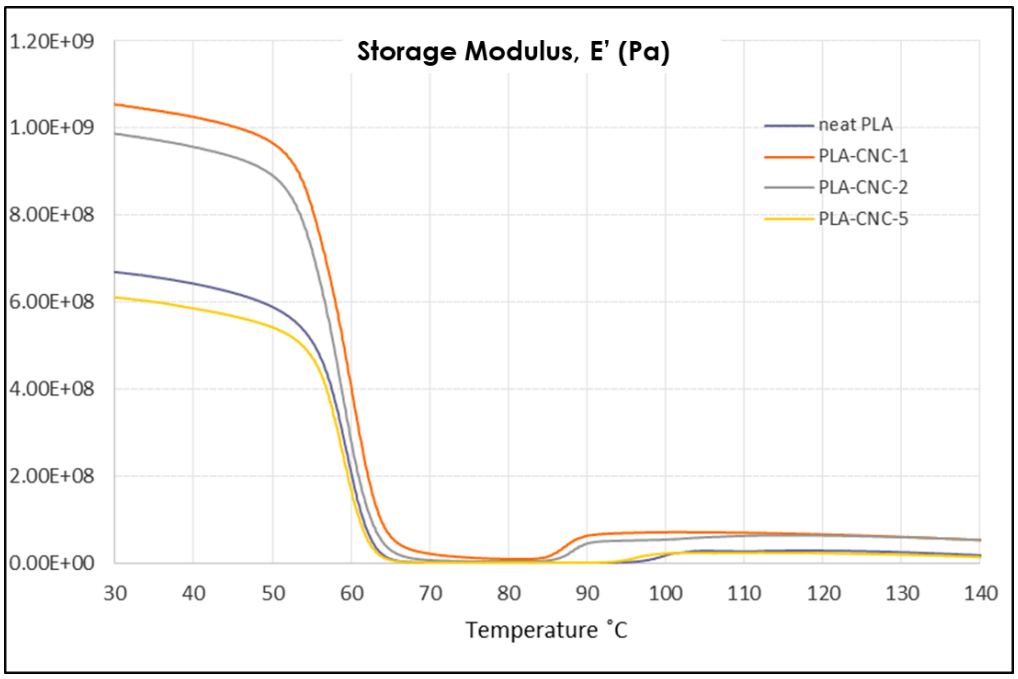

Figure 32: Storage modulus (E') as function of temperature

The loss modulus E" is also measured by DMA test, which is the measure of the viscous respond of the polymer. The values obtained from the experiment at 30˚C indicate that PLA-1 dissipate more energy since it has higher value. E" for PLA-1 is 9.14 MPa compared to neat PLA where E" is 9.10 MPa, Figure [33]. The same behavior as storage modulus is observed in loss modulus where PLA-2 and PLA-5 have lower values, 8.59 MPa and 6.95 MPa respectively.

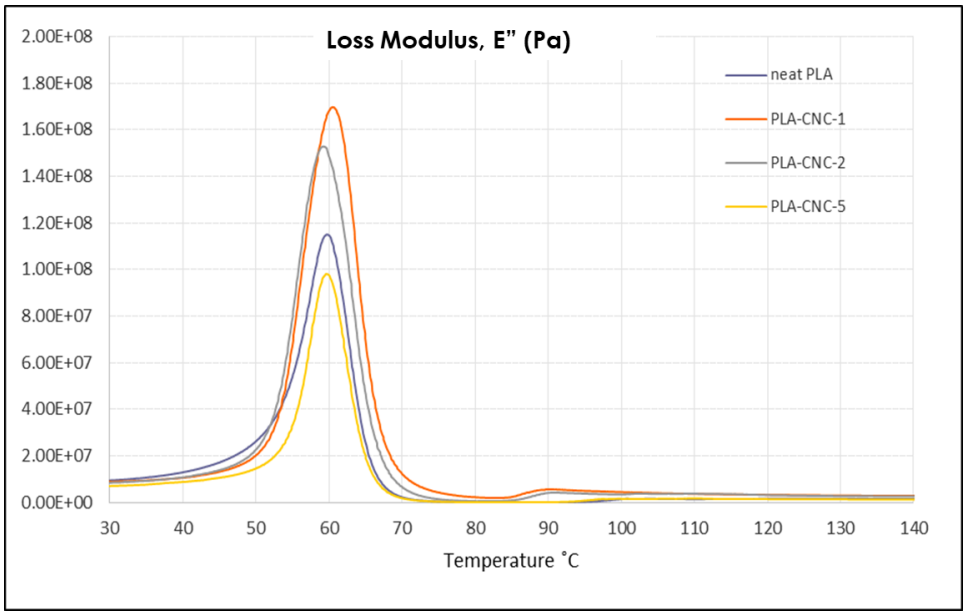

Figure 33: Loss modulus (E") vs temperature

Another important information obtained from DMA tests is tan δ, which is the relation between the storage and loss moduli. Tan δ is the ratio of viscous to elastic response of the material. It can be calculated as the ratio of loss modulus to storage modulus [$\tan\delta = \frac{E''}{E'}$]. Low value of tan δ like the one in PLA-1 indicates that the material has more potential to store the load rather than dissipate energy. Whereas for higher values in tan δ such as PLA-2 and PLA-5 shows that the material dissipates more energy. In low concentration of cellulose in the matrix, nanoparticles have better interaction with polymer chains resulting in more elastic response. However, at higher concentrations the dispersion of nanocrystals in PLA matrix is poor which restrict the polymer motion and cause an increase in tan δ value, Figure [34].

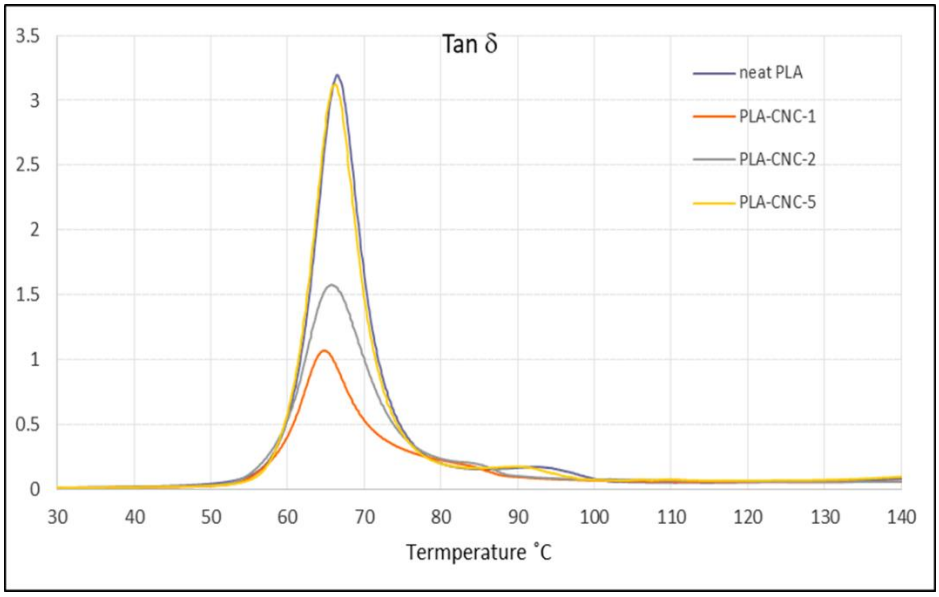

Figure 34: tan δ as function of temperature

The values of storage modulus, loss modulus and tan δ peaks are represented in the table below.

Table 8: DMA test results

	Storage modulus E' (GPa)	Loss modulus E" (MPa)	Tan δ
Neat PLA	0.68	9.10	1.58
PLA-1	1.06	9.14	1.06
PLA-2	0.95	8.59	3.20
PLA-5	0.62	6.95	3.17

Another data that can be interpreted from the DMA test is the glass transition temperature. For the four samples tested, the values of T_g are around 60˚C. These data confirm the values obtained from the DSC for the same polymer composites.

VIII. Conclusions

The aim of this work was to study the capability of preparing biopolymer nanocomposites consisting of a polylactic acid matrix reinforced with cellulose nanocrystals using single-screw extruder. The filament produced from the specified extrusion lab set-up showed good quality in nanocomposites. Utilization of Filabot spooler along with OptoControl micrometer helped to maintain the desired filament specifications while extruding. The preliminary results indicate that polymer nanocomposite can be achieved with direct mechanical mixing of PLA and CNC. Enhancement has been noticed in the mechanical properties of 1 wt% cellulose composites. The tensile strength increased by 18% compared to neat PLA, and the tensile modulus increased by 50%. The strain of the material decreases from 8.7% in neat PLA to 2.8% in PLA-1 which indicates a stiffer material. The DSC results showed that cellulose nanoparticles act as crystallization nucleating agents as a significant increase in degree of crystallinity was observed. Also, bigger crystallites were expected to form since PLA-1 has higher melting temperature (168˚C) than neat PLA (150˚C). However, increasing the cellulose concentration was detrimental to the mechanical properties of the nanocomposites. Modulus, tensile strength, and elongation to break all decreased at higher CNC contents. Poor dispersion of CNC in polymer matrix is suspected.

A. Recommendation for Future Work

1. Surface Treatment of Cellulose Nanocrystals

The obtained results from the study show that the dispersion of cellulose nanoparticles in the polymer matrix is poor. The main problem of this composite is that CNC is hydrophilic and PLA is hydrophobic which makes it difficult for both materials to interact with each other. To encounter this issue, surface treatment of cellulose nanoparticle could be applied. Several studies showed that modification of cellulose surface improved the dispersion of particle within the polymer matrix [3]. Also, the modified cellulose showed better mechanical properties when tested [4].

2. Biodegradability of Polymer Bio-composite

Polylactic acid and cellulose are natural polymers produced from natural resources. Since recycling of plastic is not an easy process, producing natural polymer would help to minimize the environmental impact of such materials. PLA degradation process was reported to be very slow, wither it was studied via hydrolysis or oxidation [20]. Improvement of degradation process was observed by several studies when nanocomposites were used [Sinha Ray, 21]. For future work, good topic of study would be the measurement of degradation of PLA/CNC nanocomposite.

3. Advanced Microscopy Investigation

Microscopy analysis is essential to understand the nanostructure of the polymer composite. The interaction between CNC and PLA could be investigated better with advanced microscopy analysis like Transmission electron microscopy (TEM). Also, TEM could be used to inspect the dispersion of cellulose nanoparticles in the matrix, signs of

agglomeration or poor dispersion could be detected via TEM. Scanning electron microscopy (SEM) is another microscopic technique used to study the surface topography. The surface of cellulose particle could be studied in the fractured surface of tensile specimens or in the filament itself. The presence of cellulose aggregates and its size can give clear picture of the dispersion within the matrix.

4. Modifications to the current extrusion set-up

The extrusion set-up used in this work presented good results in low concentration of cellulose nanocrystals in polymer matrix. However, the increase in nanofiller concentration is suspected to hinder the mechanical properties of nanocomposites. To encounter this issue, twin-screw extrusion process could be implemented instead of single-screw. The twin-screw extrusion provides better mixing between CNC and polymer matrix along with precise control of degree of mixing. Also, it provides higher level of process flexibility due to the independency of throughput to screw speed. Considering these advantages, using twin-screw extruder might enhance the processing of higher concentration of cellulose in PLA matrix.

5. Improvement of filament quality

As discussed earlier, filament quality in terms of diameter and shape is essential for the 3D printing process. The filament obtained in this work was good enough to be printed and tested, but that was not the case for all nanocomposites. It was observed that high concentration od cellulose content requires optimum drying before extruding to eliminate air bubbles in the filament. It is recommended to dry CNC and PLA powder separately before mixing them and then dry the mixture for a second time. Also, the extrusion process should follow the drying immediately to minimize the time of exposure to moisture in the

air (since the hopper is open to atmosphere). Water bath was used as cooling media during this work, it was observed that water cools down PLA filament to a temperature close or lower that T_g which makes it difficult to process. Stiffer filament is harder to manipulate and control before attach it to the spooler. After several trials, it turns out that air cooling is sufficient and produces better filament. It is recommended to install a path wheel halfway between the extruder and spooler to prevent filament wobbling and provide support. The online diameter measurement via optical micrometer showed disturbance in reading when the filament is shaking, installing the guiding wheel could help to minimize this disturbance.

References

1. Murphy, C. A., & Collins, M. N. (2016). Microcrystalline cellulose reinforced polylactic acid biocomposite filaments for 3D printing. Polymer Composites.

2. Gwon, J. G., Cho, H. J., Chun, S. J., Lee, S., Wu, Q., Li, M. C., & Lee, S. Y. (2016). Mechanical and thermal properties of toluene diisocyanate-modified cellulose nanocrystal nanocomposites using semi-crystalline poly (lactic acid) as a base matrix. RSC Advances, 6(77), 73879-73886.

3. Jonoobi, M., Harun, J., Mathew, A. P., & Oksman, K. (2010). Mechanical properties of cellulose nanofiber (CNF) reinforced polylactic acid (PLA) prepared by twin screw extrusion. Composites Science and Technology, 70(12), 1742-1747.

4. Oksman, K., Mathew, A. P., Bondeson, D., & Kvien, I. (2006). Manufacturing process of cellulose whiskers/polylactic acid nanocomposites. Composites science and technology, 66(15), 2776-2784.

5. Frone, A. N., Panaitescu, D. M., Chiulan, I., Nicolae, C. A., Vuluga, Z., Vitelaru, C., & Damian, C. M. (2016). The effect of cellulose nanofibers on the crystallinity and nanostructure of poly (lactic acid) composites. Journal of materials science, 51(21), 9771-9791.

6. Garlotta, D. (2001). A literature review of poly (lactic acid). Journal of Polymers and the Environment, 9(2), 63-84.

7. Tsuji, H. (2011). Poly (lactic acid): synthesis, structures, properties, processing, and applications. Wiley.

8. Clark, T. J. (2015). U.S. Patent No. WO2015113168A1. Washington, DC: U.S. Patent and Trademark Office.

9. Rojas, J., Bedoya, M., & Ciro, Y. (2015). Current trends in the production of cellulose nanoparticles and nanocomposites for biomedical applications. In Cellulose-Fundamental Aspects and Current Trends. InTech.

10. P. (n.d.). Cellulose Nanomaterials - The Process Development Center - University of Maine. Retrieved April 17, 2018, from https://umaine.edu/pdc/cellulose-nano-crystals/

11. Moon, R. J., Martini, A., Nairn, J., Simonsen, J., & Youngblood, J. (2011). Cellulose nanomaterials review: structure, properties and nanocomposites. Chemical Society Reviews, 40(7), 3941-3994.

12. Nishino, T., Takano, K., & Nakamae, K. (1995). Elastic modulus of the crystalline regions of cellulose polymorphs. Journal of Polymer Science Part B: Polymer Physics, 33(11), 1647-1651.

13. Raquez, J. M., Habibi, Y., Murariu, M., & Dubois, P. (2013). Polylactide (PLA)-based nanocomposites. Progress in Polymer Science, 38(10-11), 1504-1542.

14. Sperling, L. H. (2005). Introduction to Physical Polymer Science, Fourth Edition, 110-112.

15. Nam, J. Y., Sinha Ray, S., & Okamoto, M. (2003). Crystallization behavior and morphology of biodegradable polylactide/layered silicate nanocomposite. Macromolecules, 36(19), 7126-7131.

16. Ljungberg, N., & Wesslén, B. (2005). Preparation and properties of plasticized poly (lactic acid) films. Biomacromolecules, 6(3), 1789-1796.

17. Tserki, V., Zafeiropoulos, N. E., Simon, F., & Panayiotou, C. (2005). A study of the effect of acetylation and propionylation surface treatments on natural fibres. Composites Part A: applied science and manufacturing, 36(8), 1110-1118.

18. Petersson, L., Kvien, I., & Oksman, K. (2007). Structure and thermal properties of poly (lactic acid)/cellulose whiskers nanocomposite materials. Composites Science and Technology, 67(11-12), 2535-2544.

19. Chilson, L. (2011). [online] ProtoParadigm. Available at: http://www.protoparadigm.com/blog/2011/11/filament-tolerances-and-print-quality, November 29, 2011.

20. Auras, R. A., Lim, L. T., Selke, S. E., & Tsuji, H. (Eds.). (2011). Poly (lactic acid): synthesis, structures, properties, processing, and applications (Vol. 10). John Wiley & Sons.

21. Sinha Ray, S., Yamada, K., Okamoto, M., & Ueda, K. (2002). Polylactide-layered silicate nanocomposite: a novel biodegradable material. Nano Letters, 2(10), 1093-1096.

Vita

Osama Khayat was born in Al-laith which is a small village in Saudi Arabia. He is the son of Mohammad Khayat and Amnah Hafiz. He was raised in Makkah and graduated from high school in 2007 and admitted to King Fahd University of Petroleum and Minerals (KFUPM) to study chemical engineering in Dhahran, Saudi Arabia. In 2012, he graduated with a Bachelor of Science Degree in chemical engineering with second honor award. Right after that, he joined Saudi Aramco to start his first job as process engineer in Chemical Business Department. Osama worked in Yanbu Refinery in naphtha treatment and platforming unit for two years in an assignment. After that, he worked for another assignment in PetroRabigh (a joint venture of Saudi Aramco) in the ethane cracker unit where he was exposed into petrochemical industry. In 2016, he was granted a scholarship from Saudi Aramco to continue his graduate studies and he joined Lehigh University. Osama was awarded his Master of Science Degree in Polymer Science and Engineering from Lehigh University in Spring of 2018.